

## MIT Open Access Articles

*Interactions between oxygen permeation and homogeneous-phase fuel conversion on the sweep side of an ion transport membrane*

The MIT Faculty has made this article openly available. **Please share** how this access benefits you. Your story matters.

**Citation:** Hong, Jongsup, Patrick Kirchen, and Ahmed F. Ghoniem. "Interactions Between Oxygen Permeation and Homogeneous-Phase Fuel Conversion on the Sweep Side of an Ion Transport Membrane." *Journal of Membrane Science* 428 (February 2013): 309–322.

**As Published:** <http://dx.doi.org/10.1016/j.memsci.2012.10.055>

**Publisher:** Elsevier

**Persistent URL:** <http://hdl.handle.net/1721.1/99223>

**Version:** Author's final manuscript: final author's manuscript post peer review, without publisher's formatting or copy editing

**Terms of use:** Creative Commons Attribution-Noncommercial-NoDerivatives



# INTERACTIONS BETWEEN OXYGEN PERMEATION AND HOMOGENEOUS-PHASE FUEL CONVERSION ON THE SWEEP SIDE OF AN ION TRANSPORT MEMBRANE

Jongsup Hong, Patrick Kirchen, Ahmed F. Ghoniem \*

*Department of Mechanical Engineering, Massachusetts Institute of Technology,*

*77 Massachusetts Avenue, Cambridge, MA 02139, USA*

**Key Words:** Ion transport membrane; High temperature membrane reactor; Oxy-fuel combustion; Partial oxidation of methane; Syngas production; Fuel conversion; Oxygen permeation.

---

## ABSTRACT

The interactions between oxygen permeation and homogeneous fuel oxidation reactions on the sweep side of an ion transport membrane (ITM) are examined using a comprehensive model, which couples the dependency of the oxygen permeation rate on the membrane surface conditions and detailed chemistry and transport in the vicinity of the membrane. We assume that the membrane surface is not catalytic to hydrocarbon or syngas oxidation. Results show that increasing the sweep gas inlet temperature and fuel concentration enhances oxygen permeation substantially. This is accomplished through promoting oxidation reactions (oxygen consumption) and the transport of the products and reaction heat towards the membrane, which lowers the oxygen concentration and increases the gas temperature near the membrane. Faster reactions at higher fuel concentration and higher inlet gas temperature support substantial fuel conversion and lead to a higher oxygen permeation flux without the contribution of surface catalytic activity. Beyond a certain maximum in the fuel concentration, extensive heat loss to the membrane (and feed side) reduces the oxidation kinetic rates and limits oxygen permeation as the reaction front reaches the membrane. The sweep gas flow rate and channel height have moderate impacts on oxygen permeation and fuel conversion due to the residence time requirements for the chemical reactions and the location of the reaction zone relative to the membrane surface.

---

\* Corresponding author. Tel.: +1 617 253 2295; Fax: +1 617 253 5981  
Email address: [ghoniem@mit.edu](mailto:ghoniem@mit.edu) (Ahmed F. Ghoniem)

## 1. INTRODUCTION

Oxygen permeable inorganic dense membranes have been considered for simultaneous air separation and fuel conversion integrated into a single compartment. Driven by the oxygen chemical potential gradient across the membrane at high temperatures typically above 700 °C, oxygen ions selectively permeates from the air side to the sweep gas side of the membrane [1, 2]. A reactive gas such as methane can be introduced into the sweep side of an ion transport membrane (ITM) to promote simultaneous air separation and fuel conversion (i.e., ITM reactor). Oxygen consumption through the fuel oxidation reactions leads to a higher oxygen chemical potential gradient, raising the oxygen permeation rate, while the heat of reaction reduces the external thermal energy required to sustain a sufficiently high temperature [3]. In addition, the introduction of oxygen into the sweep side in a controlled manner allows complete or partial oxidation with oxygen in the absence of nitrogen (i.e., oxy-fuel combustion, syngas production and oxidative coupling). Multiple applications have been proposed for ITM reactors [4], such as oxy-fuel combustion, which is an attractive technology for carbon dioxide capture and storage [5, 6], and hydrocarbon reforming to produce syngas through partial oxidation, which can be used for liquid fuel synthesis or hydrogen production [7-9].

When a reactive gas is added to the sweep stream of an ITM reactor, the oxygen permeation rate and the hydrocarbon conversion are influenced by the local thermodynamic state (predominantly the oxygen concentration and the gas temperature near the membrane surface). Because oxygen is introduced through permeation, the fuel and oxidizer in the sweep side of an ITM are not pre-mixed, leading to the establishment of a non-premixed or diffusion-controlled reaction zone [10]. In such diffusion-supported reactions, the local thermodynamic state including species concentration and temperature play significant roles in establishing stable reactions and determining the reaction products. Unlike typical diffusion-controlled combustion in which the temperature is so high that the overall hydrocarbon conversion rate is governed almost solely by diffusion, the temperature in an ITM reactor is kept low to protect the membrane, and hence chemical kinetics play an important role in determining the fuel conversion rate. Furthermore, the initial conditions of the oxidizer and the fuel streams (i.e., permeated oxygen and sweep gas in the case of ITM reactors, respectively) govern the hydrocarbon conversion. However, unlike other conventional reactors, the flow rate and temperature of the oxidizer stream (i.e., oxygen permeation) in an ITM reactor are not known a priori and rather depend on the oxygen partial pressure in the immediate vicinity of the membrane and its temperature. Therefore, it is difficult to independently control the mass ratio of the fuel to the oxidizer in the sweep side and hence hydrocarbon conversion processes.

Modeling approaches implemented so far have not resolved the interdependency of oxygen permeation and the reactive flow in detail. Jin et al. [11] and Tan et al. [12] examined the dependence of the oxygen permeation rate and the CH<sub>4</sub> conversion on the operating conditions including the temperature, the air and sweep gas flow rates and the reactor geometry. They assumed a plug flow to model their reactor and negligible temperature variations due to the chemical reactions. Smit and Zhang et al. [13, 14] presented a more detailed model, but it still neglected the species transport and heat transfer from the bulk stream in the gas-phase towards the membrane surface. Tan and Li [9] resolved spatially the species concentration and temperature on the sweep side in a membrane reactor used for partial oxidation of methane. Implementing a three-step reaction mechanism, they discussed the product selectivity and hydrocarbon conversion with respect to the temperature, the fuel flow rate, the membrane tube diameter and the membrane thickness. However, their numerical model was based on an oxygen permeation rate expression parameterized in terms of the bulk stream parameters, not the local thermodynamic state at the membrane surface. Moreover, they assumed fuel conversion on the catalyst surface (mounted on the membrane) and neglected gas-phase fuel conversion processes that could lead to the local variations of species concentration and temperature along the direction normal to the membrane.

In this study, the interactions between oxygen permeation and fuel conversion on the sweep side of an ITM are investigated using numerical simulations. A computational model that resolves species concentration and temperature, spatially and temporally, is used. Detailed gas-phase chemistry and species transport are incorporated to examine the fuel conversion and mass transfer in the gas-phase, while an oxygen permeation rate expression parameterized in terms of the oxygen partial pressures on the membrane surface and the membrane temperature is applied to account for the influence of the local thermodynamic state on oxygen permeation. The parameters used in the expression, such as the diffusivity of oxygen vacancy and surface exchange rate coefficients, are based on oxygen permeation rate measurements for La<sub>0.6</sub>Sr<sub>0.4</sub>Co<sub>0.2</sub>Fe<sub>0.8</sub>O<sub>3-δ</sub> [3, 15]. It is assumed that no additional catalyst is mounted on the membrane, and the membrane surface is not catalytically active for hydrocarbon or syngas conversion. To elucidate the relationship between fuel conversion and oxygen permeation, a parametric study is performed with respect to several control parameters including the fuel concentration in the sweep gas stream (i.e., fuel plus a diluent), its inlet temperature, flow rate and the channel height (i.e., the distance from the membrane to the sweep gas inlet or the opposite walls). The numerical approach used in this study is summarized in Section 2. The parametric study results with respect to the control parameters are discussed in

Section 3. Section 4 includes discussion regarding the feedback interactions between the  $\text{CH}_4$  conversion and the oxygen permeation rate.

## 2. NUMERICAL APPROACH

Investigations on fuel conversion and oxygen permeation in an oxygen permeable mixed ionic-electronic conducting membrane reactor are conducted using numerical simulations. To examine the operating regimes of an ITM reactor, the physical model considers a planar, finite-gap stagnation-flow configuration shown in Figure 1. An experimental apparatus in our laboratory is also based on this configuration, which is described in [16]. The self-similar stagnation-flow configuration is selected because detailed chemistry and species transport in the gas-phase can be implemented while keeping the computational cost at a manageable level. Detailed analysis of the chemical reactions, the mass and heat transfer and the local thermodynamic state is necessary for the fundamental studies of ITM supported fuel conversion processes and their relationship with oxygen permeation. Although the results from this study may not be directly applicable to all reactor systems due to the geometry, the flow field (and thus the mass transfer) and reactor dynamics, this configuration allows sufficiently detailed analysis of the fluid dynamic and thermo-chemical processes, contributing to the fundamental understanding of ITM reactors and the underlying physics in multi-dimensional, commercial reactor configurations. Furthermore, the fundamental knowledge and oxygen permeation expressions gained from such investigations can be applied for future studies considering more complex reactor configurations and geometries.

The numerical model spatially resolves the gas-phase flow, transport and chemical reactions and incorporates an oxygen permeation rate expression that models both surface exchange and bulk diffusion processes to connect oxygen permeation with the gas-phase flow field. The detail of the numerical model including the governing equations, the boundary conditions at the air and sweep gas inlets and the membrane surface and the oxygen permeation rate expression were discussed in our previous study [3] and are briefly summarized here. Starting with the general three-dimensional governing equations for reacting flow [17], the dimensionality of the model is reduced to one dimension considering the similarity behavior of the flow. In the neighborhood of the stagnation line, the flow variables (i.e., density, velocity, temperature and species concentration) and their local variations can be described using a self-similar solution in the direction normal to the membrane (i.e.,  $y$ -direction). In addition, a low Mach number assumption is employed because of

low gas velocities. The pressure variations are negligible in comparison with the thermodynamic pressure, and the oxygen partial pressure depends only on its mole fraction for a given pressure. While flux-matching conditions, i.e., oxygen permeation and heat fluxes across the membrane, are applied at the membrane surface, input operating conditions, i.e., the gas composition, flow rate and temperature, are imposed at the inlets. The oxygen permeation rate expression was parameterized (i.e., the diffusivity of oxygen vacancy and surface exchange rate coefficients) in terms of the local oxygen partial pressures in the immediate vicinity of the membrane [3], as opposed to conventional expressions in which the oxygen concentration at the bulk streams measured at the air inlet and sweep gas outlet are used [15]. Since the oxygen concentration on the sweep side of an ITM varies significantly between the bulk and the membrane surface due to the chemical reactions and the mass transfer, the oxygen permeation rate expression used in the analysis must be based on the local oxygen partial pressures at the membrane surface. The expression also resolves the dependence of oxygen permeation on the membrane temperature, the local oxygen partial pressure and the membrane thickness.

To examine the fuel conversion processes, a detailed chemical kinetic mechanism for methane (GRI-Mech 3.0 [18]) is implemented for the homogeneous gas-phase chemical reactions. To integrate the multi-step chemical reactions and evaluate thermodynamic and transport properties, Cantera [19] is used along with NASA polynomials. Surface reactions are ignored to focus on the gas-phase fuel conversion and their relationship with oxygen permeation. Surface chemistry will be considered in future studies.

### 3. PARAMETRIC STUDY

To examine the interactions between fuel conversion and oxygen permeation, a parametric study is conducted with respect to several control parameters including the fuel concentration in the sweep gas stream on a molar basis,  $x_{CH_4, sweep}$ , the sweep gas inlet temperature,  $T_{sweep}$ , volumetric flow rate,  $F_{sweep}$ , and the channel height,  $H_{sweep}$ . The parameters and their variations considered in the parametric study are summarized in Table 1. The interaction between the permeated oxygen and the fuel forms a laminar, non-premixed (diffusion), oxy-fuel reaction zone [10]. The oxygen permeation rate is substantially lower than the flow rate of a convective oxidizer feed stream in conventional counter-flow diffusion flames [2, 20, 21], and hence the fuel stream (i.e., sweep gas) has to be fed into the sweep side at a low velocity in order to maintain

an overall stoichiometric mixture. Moreover, the fuel stream is heavily diluted with CO<sub>2</sub> to keep the reaction zone temperature low [22] in order to protect the membrane material, and hence the fuel oxidation kinetic rates are not as fast as in the case of conventional diffusion flames. To meet this requirement, the base-case considers a sweep gas volumetric flow rate of  $4.39 \times 10^{-4}$  m<sup>3</sup>/s (sweep gas velocity at the inlet =  $7.56 \times 10^{-2}$  m/s,  $Re_{sweep} = 15.6$ ) and a fuel concentration of 6%, with the remainder being CO<sub>2</sub> at a temperature of  $T_{sweep} = 1300K$ . Note that, integrated at the front end of a power plant, an ITM reactor may use a hot recycled carbon dioxide stream as a diluent in the sweep gas stream. The base-case considers a membrane thickness,  $L$ , of 100  $\mu$ m and the sweep gas channel height of 25.4 mm. Throughout the parametric study, the air inlet flow rate of  $1.97 \times 10^{-3}$  m<sup>3</sup>/s (air velocity at the inlet =  $3.70 \times 10^{-1}$  m/s,  $Re_{air} = 100$ ) and temperature of 1300 K, are maintained constant. It is assumed that the surrounding wall temperature is the same as the gas (i.e., both air and sweep gas) inlet temperature. The total pressure is kept constant at 1 atm. These control parameters for the base-case are selected as they are representative of realistic operating conditions for ITM reactors.

### 3.1. Base-case Results and Important Features

The base-case results highlight the characteristics of the diffusion-controlled reaction zone and the important features regarding fuel conversion and oxygen permeation. Figure 2(a) shows the variations of the CH<sub>4</sub> and O<sub>2</sub> molar concentrations, the temperature and the heat release rate between the membrane and the sweep gas inlet. The concentrations of CH<sub>4</sub> and O<sub>2</sub> decrease from the sweep gas inlet and the membrane surface, respectively, approaching the reaction zone in which the maximum temperature and the peak heat release rate are found. The chemical reactions, i.e., CH<sub>4</sub> conversion and O<sub>2</sub> consumption, around the reaction zone lower their concentrations while raising the heat release rate and the temperature. A rise in temperature exists even in regions without a significant heat release due to the heat transfer and the transport of the hot products towards both the membrane surface and the sweep gas inlet. A sharp temperature gradient near the membrane indicates a high heat transfer rate towards the membrane,  $Q_{transfer}$ , of 7.44 kW/m<sup>2</sup>, being a significant fraction of the gross heat release,  $Q_{gen}$ , of 12.1 kW/m<sup>2</sup>. This raises the membrane temperature while lowering the reaction zone temperature [10]. The membrane conducts a part of this heat (3.19 kW/m<sup>2</sup>) to the air side and transfers the rest of it (4.25 kW/m<sup>2</sup>) to the sweep side surrounding walls via radiation. On the air side, the conducted heat plus the thermal energy associated with oxygen permeation of 1.06 kW/m<sup>2</sup> is transferred towards the air side surrounding walls via radiation (4.25

kW/m<sup>2</sup>). Note that the radiative heat transfer plays an important role in controlling the membrane temperature and maintaining a high reactor temperature. The gross heat release is defined as follows,

$$Q_{gen} = \int_0^{H_{sweep}} q dy_{sweep} = \int_0^{H_{sweep}} \left( \sum_1^N \dot{\omega}_k \hat{h}_k \right) dy_{sweep} \quad (\text{Eq.1})$$

where  $q$  is the heat release rate;  $N$  is the number of gas-phase species;  $\dot{\omega}_k$  is the molar production rate of species  $k$ ;  $\hat{h}_k$  is the molar enthalpy of species  $k$ . The gross heat release shows the extent of the chemical reactions and their effect on the temperature rise, whereas the heat transfer to the membrane indicates a thermal effect on the temperature drop.

The transport of the products away from the reaction zone is also important for determining the temperature as well as the local species concentration. The major products from fuel conversion processes include CO<sub>2</sub>, CO, H<sub>2</sub> and H<sub>2</sub>O, and their concentrations indeed show large increase around the reaction zone (i.e., production) and continuous reductions away from it (i.e., transport), as shown in Figure 2(b). Note that the CO<sub>2</sub> concentration drops as the fuel stream reaches the reaction zone increasing that of CO, due to decomposition or reverse water gas-shift reactions, which suppresses the production of H<sub>2</sub> [10, 23]. The reduction in the CO<sub>2</sub> concentration is also attributed to the transport of O<sub>2</sub> and H<sub>2</sub>O towards the sweep gas inlet. After being produced through the chemical reactions, the primary products diffuse out from the reaction zone towards the membrane surface and the sweep gas inlet. Thus, in such diffusion-controlled reactions, both species production and their transport are important for determining the local thermodynamic state including species concentration and temperature. In particular, when comparing the molar concentration of the products and oxygen at the membrane surface in Figure 2(a) and Figure 2(b), it can be seen that the transport of the products towards the membrane surface reduces the oxygen concentration and raises the gas temperature near the membrane. Since the reaction zone, the location of which, relative to the membrane, is represented by the location (i.e., reaction front,  $y_{front}$ ) of the maximum heat release rate, is established near the membrane surface, the effect of species transport towards the membrane is substantial, resulting in a low oxygen partial pressure in the immediate vicinity of the membrane,  $P_{O_2,mem}$ , and a high membrane temperature,  $T_{mem}$ . As a result, the transport of the products and heat towards the membrane along with oxygen consumption through the chemical reactions enhances the oxygen permeation rate,  $J_{O_2}$ , to 3.53  $\mu\text{mol}/\text{cm}^2/\text{s}$ , in comparison



with the case of an inert sweep gas which achieves the oxygen permeation rate less than or nearly  $1.00 \mu\text{mol}/\text{cm}^2/\text{s}$  [3]. The transport of the reaction products towards the membrane is also important in influencing the kinetic rates on the oxidizer side of a diffusion-controlled reaction zone. The product concentrations on the oxidizer side of a reaction zone can change substantially the  $\text{O}_2$  consumption and radical reaction rates, i.e., chain-branching and chain-terminating reactions [10]. Moreover, depending on the membrane, the composition of the mixture at the membrane surface can have significant implications on the membrane longevity [24-26].

Fuel conversion processes in an ITM reactor can be characterized by key variables such as the  $\text{CH}_4$  conversion, the gross heat release, the residence time and the average scaled transverse (i.e., parallel to the membrane) velocity. The  $\text{CH}_4$  conversion,  $X_{\text{CH}_4}$ , is defined as,

$$X_{\text{CH}_4} = \frac{V_{\text{CH}_4, \text{converted}}}{(F_{\text{sweep}} x_{\text{CH}_4, \text{sweep}} \zeta_{\text{sweep}}) / A_{\text{sweep}}} = \frac{\int_0^{H_{\text{sweep}}} -\dot{\omega}_{\text{CH}_4} dy_{\text{sweep}}}{(F_{\text{sweep}} x_{\text{CH}_4, \text{sweep}} \zeta_{\text{sweep}}) / A_{\text{sweep}}} \quad (\text{Eq.2})$$

where  $V_{\text{CH}_4, \text{converted}}$  is the conversion rate of  $\text{CH}_4$  on the sweep side;  $\zeta_{\text{sweep}}$  is the molar density of the sweep gas;  $A_{\text{sweep}}$  is the sweep gas inlet area. The  $\text{CH}_4$  conversion indicates how much fuel is consumed relative to the amount of fuel in the sweep gas stream, representing the effectiveness of fuel conversion processes on the sweep side. The base-case result shows a  $\text{CH}_4$  conversion of 39.4%. The rest of the fuel cannot be converted through the chemical reactions and rather flows out from the reaction zone following the transverse velocity, whose magnitude is represented by the average scaled transverse velocity,  $U_{\text{avg}}$ :

$$U_{\text{avg}} = \frac{1}{H_{\text{sweep}}} \int_0^{H_{\text{sweep}}} U dy_{\text{sweep}} \quad (\text{Eq.3})$$

where  $U$  is the scaled transverse velocity (see Figure 1). Given the normal velocities of the oxidizer (i.e., oxygen permeation at the membrane surface) and the fuel (i.e., sweep gas at the inlet) streams and the sweep gas channel height, the flow field within the sweep side is determined and hence the transverse velocity. In addition, the normal velocities of both

streams determine the available time or the residence time for the chemical reactions. The residence time,  $t_{res}$ , is defined as,

$$t_{res} = \frac{H_{sweep}}{(v_{O_2} + v_{sweep})} \quad (\text{Eq.4})$$

where  $v_{O_2}$  is the velocity associated with the oxygen permeation rate;  $v_{sweep}$  is the sweep gas velocity at the sweep gas inlet. Under diffusion-controlled conditions, the fuel oxidation kinetics governs the  $\text{CH}_4$  conversion based on such variables as the flow field as well as the local thermodynamic state and the initial conditions of the oxidizer and the fuel streams.

Important features found in the base-case results show that it is worthwhile to investigate the relationship between fuel conversion and oxygen permeation by varying flow conditions on the sweep side. In diffusion-controlled reactions, the local thermodynamic state has a large impact on the fuel oxidation kinetics and hence the  $\text{CH}_4$  conversion. Furthermore, oxygen consumption via the chemical reactions, the species transport and heat transfer towards the membrane play significant roles in determining the gas temperature and the oxygen concentration in the vicinity of the membrane, affecting the oxygen permeation rate. For these reasons, a parametric study is conducted with respect to the control parameters that change flow conditions on the sweep side, including the fuel concentration in the sweep gas, its inlet temperature, flow rate and the channel height.

### 3.2. Effect of Fuel Concentration

In an ITM reactor used for oxy-fuel combustion or fuel reforming, the fuel is diluted in  $\text{CO}_2$ . Here, we investigate the impact of the fuel concentration in the  $\text{CO}_2$  sweep stream on fuel conversion and oxygen permeation. In the parametric study, the fuel concentration is raised from 3% to 30%, while the sweep gas inlet temperature, flow rate and channel height are maintained at their base-case values. Figure 3 shows that increasing the fuel concentration enhances the oxygen permeation rate substantially up to  $x_{\text{CH}_4, \text{sweep}} \approx 15\%$ , while the  $\text{CH}_4$  conversion is gradually lowered. Beyond this point, as the fuel concentration is raised further, the oxygen permeation rate starts decreasing. As the oxygen permeation rate approaches a peak, the  $\text{CH}_4$  conversion does not change significantly, but decreases extensively again, as the oxygen

permeation rate decreases with further increases in fuel concentration. To examine why these two regimes (i.e., the enhancement and reduction of the oxygen permeation rate) exist, variables changing largely with the fuel concentration and affecting the oxygen permeation rate and the CH<sub>4</sub> conversion need to be investigated.

Oxygen consumption, the generation and transport of the products, in particular, the primary products such as H<sub>2</sub>O, near the membrane and the heat transfer towards it play significant roles in determining the oxygen permeation rate through the oxygen partial pressure near the membrane and its temperature. In addition, the reaction zone is shifted towards the membrane with increasing CH<sub>4</sub> concentration, which further lowers the CH<sub>4</sub> conversion. Figure 4(a) shows the enhancement of the oxygen consumption rate,  $\dot{\omega}_{O_2}$ , and the gross heat release with the fuel concentration. In addition, as the fuel concentration is raised, the reaction zone is shifted towards the membrane, while the molar flow rate ratio of the oxygen permeation rate to the fuel influx,  $J_{O_2} / J_{CH_4, in}$ , gradually decreases. Higher reactant concentrations in the reaction zone promote the fuel oxidation kinetics in the gas-phase, consuming more oxygen, and result in substantial fuel conversion, although the membrane is not catalytically active. Furthermore, since the increase in oxygen permeation is not sufficient to match that of the fuel supply, raising the fuel concentration moves the reaction zone towards the oxidizer stream inlet, i.e., the membrane surface. As such, more fuel is convected out following the transverse velocity prior to the reaction zone, hence reducing the CH<sub>4</sub> conversion. On the other hand, when the reaction zone is shifted towards the membrane along with the higher oxidation kinetic rates, more products such as H<sub>2</sub>O are produced and transported towards the membrane, increasing the product concentration at the membrane surface while decreasing that of O<sub>2</sub>, as shown in Figure 4(b). In the meantime, the heat transfer increases significantly driven by a larger gross heat release and the reaction zone established closer to the membrane, which leads to a higher membrane temperature. Therefore, the enhancement of oxygen consumption, species production and transport near the membrane and the heat transfer lowers the oxygen partial pressure in the immediate vicinity of the membrane and increases its temperature, hence enhancing the oxygen permeation rate. However, these variations change their trends as the reaction zone reaches the membrane. Once this occurs, subsequent increases in the fuel concentration result in decreases in the oxygen permeation rate.

The heat transfer towards the membrane impacts the reaction zone temperature and the fuel oxidation kinetics, and causes the reaction zone remaining near the membrane surface. The maximum gas temperature,  $T_{max}$ , represents the

reaction zone temperature. Figure 5(a) shows that the reaction zone temperature initially increases with the fuel concentration. However, as the fuel concentration is raised, the reaction zone temperature reaches a peak at the same fuel concentration at which the net heat release (gross heat release minus heat transfer) is at a maximum. It should be noted that this occurs at a lower fuel concentration than the maximum gross heat release. In addition, the concentrations of the reactants such as CH<sub>4</sub>, CO and H<sub>2</sub> at the membrane surface rise slowly, when the reaction zone temperature decreases substantially with a further increase of the fuel concentration. When the gross heat release increases with the fuel concentration, the heat transfer also increases resulting in the reduction of the net thermal energy released,  $Q_{gen} - Q_{transfer}$ , which contributes to the variation of the reaction zone temperature. When the reaction zone is established close to the membrane, heat transfer to the air side and reactor walls increases, and extensive heat loss lowers the reaction zone temperature significantly. This slows down the fuel oxidation kinetics, and eventually leads to the reaction zone remaining near the membrane surface [27, 28]. Figure 5(b) shows the heat release rate profiles at different fuel concentrations, showing that the reaction zone reaches the membrane, and the maximum heat release rate reduces at high fuel concentration. As a result of extensive heat loss and the reaction front remaining at the membrane surface, when the fuel concentration is further increased, partial oxidation of methane, CO<sub>2</sub> decomposition reactions or the reverse water gas-shift reactions and hydrocarbon pyrolysis prevail, and the extent of the chemical reactions is reduced, while the reactants that are not fully oxidized reach the membrane surface. Therefore, at high fuel concentration, the oxygen permeation rate is reduced due to the lower kinetic rate of oxygen consumption and associated increase in local oxygen concentration and the reduced generation and transport of the products near the membrane and the heat transfer, all due to the reaction zone being located at the membrane surface. The rise in the reactant concentrations at the membrane surface implies that heterogeneous chemistry may play a role at high fuel concentration if the catalytic activity of the membrane is significant or if it has additional catalysts on its surface.

The heat loss to the air side and the surrounding walls via radiation from the membrane limits the rise of the membrane temperature and its effect on oxygen permeation. As shown in Figure 4(b), the variation of the membrane temperature is much smaller than that of the reaction zone temperature (see Figure 5(a)). Although a substantial amount of thermal energy is transferred to the membrane from the sweep side due to the chemical reactions, as the reaction zone is shifted towards the membrane, the rise of the membrane temperature is insignificant. This is attributed to the extensive heat loss to the air side and the surrounding walls via surface radiation. Note that the membrane sees large surrounding walls

whose temperatures are maintained at the gas inlet temperature, as shown in Figure 1. Since the membrane temperature is nearly constant, its effect on oxygen permeation is limited, and the oxygen permeation rate is mostly dependent on the oxygen partial pressure. As seen in Figure 3 and Figure 4(b), the oxygen permeation rate increases nearly three-fold, as the oxygen concentration near the membrane surface is significantly reduced for increasing fuel concentrations (given that the reaction zone is not at the membrane surface). At a high membrane temperature, oxygen permeation is largely governed by the species concentration in the vicinity of the membrane. Thus, the species concentration near the membrane surface and the location of the reaction zone relative to the membrane play important roles in controlling oxygen permeation.

### 3.3. Effect of Sweep Gas Inlet Temperature

The sweep gas inlet temperature is another important parameter that is expected to impact oxygen permeation and fuel conversion. To examine its effect, the sweep gas inlet temperature is varied from 1050 K to 1400 K while maintaining the fuel concentration, the sweep gas flow rate and channel height at their base-case values. The air inlet and reactor wall temperature are also changed to the same value. As discussed in [3], the oxygen permeation rate varies significantly depending on the membrane temperature, and a higher sweep gas inlet temperature raises the membrane temperature, enhancing oxygen permeation. Figure 6 shows that, as the sweep gas inlet temperature is increased, the oxygen permeation rate first grows slowly and then experiences a sudden and significant increase around  $T_{sweep} \approx 1200\text{ K}$  at which the  $\text{CH}_4$  conversion also rises substantially. Beyond this point, as the sweep gas inlet temperature is raised further, the growth rate of the oxygen permeation rate is lowered, while the  $\text{CH}_4$  conversion keeps increasing extensively. To investigate why these sudden and substantial increases of the oxygen permeation rate and the  $\text{CH}_4$  conversion occur and their growth rates change, variables that depend on the sweep gas inlet temperature and impact oxygen permeation and fuel conversion are examined.

The onset of homogeneous fuel oxidation reactions contributes to the consumption of the permeated oxygen and the generation and transport of species near the membrane. Figure 7(a) shows that the gross heat release and the oxygen consumption rate rise substantially around  $T_{sweep} \approx 1200\text{ K}$ , which coincides with the increase of the oxygen permeation rate and the  $\text{CH}_4$  conversion, as the sweep gas inlet temperature is raised. This phenomenon can be explained by the initiation of the  $\text{CH}_4$  oxidation kinetics. When the gas temperature is not high enough to facilitate methane oxidation, only the decomposition of  $\text{CH}_4$  and  $\text{CO}_2$  occurs, which does not significantly affect the oxygen concentration or temperature and,

as such, does not impact the oxygen permeation. To obtain the considerable gas-phase fuel conversion and oxygen permeation from the ITM reactor, the sweep gas inlet temperature has to be high enough, i.e., above an ignition temperature at the given reactant concentration, to facilitate the  $\text{CH}_4$  oxidation reactions. Note that the typical operating temperature or membrane temperature of ITM reactors are high enough to permeate substantial oxygen to the sweep side in order to enable fuel conversion processes [2]. As a result, in the case of ITM reactors operating at high temperature, fuel oxidation reactions in the gas-phase can contribute substantially to the enhancement of oxygen permeation and fuel conversion. The sweep gas inlet temperature influences oxygen permeation not only by changing the membrane temperature, but also promoting fuel oxidation kinetics. However, as the sweep gas inlet temperature is raised further (after the initiation of homogeneous fuel oxidation reactions), the growth rate of the oxygen permeation rate decreases, although a higher gas temperature continues to increase the membrane temperature, enhances the fuel oxidation kinetics, and increases the oxygen permeation rate.

The reaction zone shifts away from the membrane with an increase of the oxygen permeation rate, reducing the effect of mass and heat transfer on oxygen permeation. When the temperature is significantly high and fuel oxidation occurs, a significant  $\text{H}_2\text{O}$  concentration at the membrane surface and the heat transfer towards it are obtained, lowering the oxygen partial pressure and raising the membrane temperature, which confirms the effect of the  $\text{CH}_4$  oxidation and the mass and heat transfer on oxygen permeation, as shown in Figure 7(b). However, as the sweep gas inlet temperature is raised further, the  $\text{H}_2\text{O}$  concentration near the membrane and the heat transfer decrease slowly, although the oxidation reactions are further promoted, as the reaction zone is pushed away from the membrane due to a higher oxygen permeation rate. Consequently, the oxygen concentration at the membrane surface grows gradually, driven by a higher oxygen permeation rate. The heat and mass transfer towards the membrane is reduced when the reaction zone is established further from the membrane, which weakens their effect to lower the  $\text{O}_2$  concentration in the vicinity of the membrane and to raise its temperature. Because of the reduced mass transfer, the accumulation of the permeated oxygen on the sweep side reduces the growth rate of oxygen permeation, as the sweep gas inlet temperature is raised further after the onset of homogeneous fuel oxidation reactions. Therefore, oxygen permeation is governed not only by oxygen consumption, but also by the heat and mass transfer.

### **3.4. Effect of Sweep Gas Flow Rate**

We now examine the influence of another sweep gas inlet condition, the sweep gas volumetric flow rate, which determines the effect of fuel stream velocity on fuel conversion and oxygen permeation. The change in the sweep gas flow rate influences the flow field and hence the mass transfer. To highlight the mass transfer effect, the sweep gas flow rate is varied from  $3.00 \times 10^{-4} \text{ m}^3/\text{s}$  to  $4.50 \times 10^{-3} \text{ m}^3/\text{s}$  while maintaining the fuel concentration in the sweep gas stream, its inlet temperature and the channel height at their base-case values. Figure 8 shows that, as the sweep gas flow rate is raised, the  $\text{CH}_4$  conversion gradually decreases, whereas the oxygen permeation rate increases, before showing sudden and substantial reductions around  $F_{\text{sweep}} \approx 2.30 \times 10^{-4} \text{ m}^3/\text{s}$ . Beyond this point, the oxygen permeation rate is raised again with an increase of the sweep gas flow rate, while the  $\text{CH}_4$  conversion remains negligible. Given the fuel concentration and temperature, the homogeneous fuel oxidation reactions can proceed and contribute to fuel conversion and oxygen permeation up to a certain flow rate. Beyond this flow rate, oxygen permeation is governed by a non-reacting flow. To verify the reason for these variations and the extinction of fuel conversion processes in the gas-phase, variables that have impacts on the oxygen permeation rate and the  $\text{CH}_4$  conversion when the sweep gas flow rate is raised are examined.

The enhanced species transport establishes the reaction zone closer to the membrane and contributes to an increase of the oxygen permeation rate, but reduces  $\text{CH}_4$  conversion. Figure 9(a) shows that the reaction zone is gradually shifted towards the membrane, and the  $\text{CO}_2$  concentration in the immediate vicinity of the membrane rises, leading to the reduction of the oxygen partial pressure near it to a similar degree, with an increase of the sweep gas flow rate. The  $\text{H}_2\text{O}$  concentration at the membrane surface remains constant and then decreases to a small value, approximately  $F_{\text{sweep}} \approx 2.30 \times 10^{-4} \text{ m}^3/\text{s}$ , coinciding with the significant reductions of both the oxygen permeation rate and the  $\text{CH}_4$  conversion. A higher sweep gas flow rate enhances the convective transport of the species towards the membrane and results in the reaction zone being established closer to it. In this case, more species such as  $\text{CO}_2$  are transferred towards the membrane surface, which lowers the concentration of  $\text{O}_2$  in the vicinity of the membrane, hence increasing the oxygen permeation rate. However, the concentration of  $\text{H}_2\text{O}$  at the membrane surface does not change even with the movement of the reaction zone towards the membrane and a larger oxygen permeation rate, which promotes the formation of the products. This is attributed to the limited enhancement of homogeneous fuel oxidation reactions, as evidenced by the small rise of the gross heat release and the  $\text{O}_2$  consumption rate shown in Figure 9(b), and the low fuel concentration. In the meantime, the heat transfer towards the membrane increases more substantially, driven by the displacement of the reaction

zone, as the sweep gas flow rate is raised. Aided by the rise of the permeated oxygen, the fuel oxidation reactions are promoted, forming more products and consuming oxygen, which also contributes to an increase of the oxygen permeation rate. However, despite the rise of the oxygen permeation rate, the growth of the gross heat release is not significant. In addition, the low  $\text{CH}_4$  concentration leads to a small increase in the  $\text{H}_2\text{O}$  concentration, and the overall reactions are predominantly governed by the  $\text{CO}/\text{CO}_2$  reactions due to a high  $\text{CO}_2$  concentration on the sweep side [10]. Thus, the limited enhancement of the fuel oxidation reactions in the gas-phase and the low fuel concentration increase the formation of the reaction products slowly, as compared to the faster transport of  $\text{CO}_2$ , the net effect of which is that the  $\text{H}_2\text{O}$  concentration at the membrane surface is approximately constant. The slowly promoted oxidation reactions, a gradual reduction in the molar flow rate ratio of the permeated oxygen to the fuel influx and the movement of the reaction zone towards the membrane contribute to a continuous reduction in  $\text{CH}_4$  conversion before the extinction of the fuel oxidation reactions.

The limited enhancement of the chemical reactions and their extinction are attributed to the higher heat capacity of the sweep gas due to the higher flow rate, as well as to the extensive heat loss towards the membrane, the smaller residence time and the flow field with a higher transverse velocity. Figure 9(c) shows that, as the sweep gas flow rate is increased, the residence time and the reaction zone temperature are gradually reduced, while the average scaled transverse velocity increases significantly. Since the velocity associated with oxygen permeation is approximately three orders of magnitude smaller than the sweep gas velocity at the inlet due to the low oxygen permeation rate [10], the residence time is predominantly governed by the sweep gas velocity, i.e., the sweep gas flow rate. Given the sweep gas channel height, a higher sweep gas velocity results in a smaller residence time (see Eq.4) and a flow field that is more stretched in the direction parallel to the membrane gaining a higher transverse velocity. In this case, a substantial fraction of the fuel is not converted and rather flows out from the reaction zone, and the convective heat transfer away from the reaction zone is enhanced. In addition, the heat capacity of the sweep gas is raised due to a higher sweep gas flow rate, as is the convective heat transfer to the membrane, both of which reduce the temperature rise driven by the reaction exothermicity, even if the gross heat release is increased. Note that the extinction of the homogeneous oxidation reactions coincides nearly with the flow rate at which the reaction zone reaches the membrane (compare Figure 9(a) and Figure 9(b)), which highlights the significant effect of the heat transfer towards the membrane on fuel conversion processes. As a result, the oxidation kinetic rates are substantially lowered. If the sweep gas velocity is too high such that the residence time is not sufficient for the fuel oxidation kinetics, the homogeneous fuel oxidation reactions cannot proceed. As a result of this mass and heat transfer



effect, the chemical reactions in the gas-phase are extinguished with an increase of the sweep gas flow rate, and their positive effect on oxygen permeation and fuel conversion vanishes.

### 3.5. Effect of Sweep Gas Channel Height

It has been shown above that the location of the reaction zone relative to the membrane and the flow field play important roles in determining the oxygen permeation rate and the CH<sub>4</sub> conversion. Now we investigate another way to manipulate them. The flow field and reaction zone position can be manipulated without changing the sweep flow rate or fuel concentration, both of which have significant impacts on the kinetics of fuel conversion, by varying the sweep gas channel height. In the following, the sweep gas channel height is varied from 3 mm to 30 mm while maintaining the fuel concentration in the sweep gas stream, the inlet temperature and flow rate at their base-case values. Figure 10 shows that, as the sweep gas channel height is reduced, the oxygen permeation rate and the CH<sub>4</sub> conversion first increase and then show substantial reductions around  $H_{sweep} \approx 7.5mm$ . When the sweep gas channel height is reduced further beyond this point, the oxygen permeation rate rises again, whereas the CH<sub>4</sub> conversion is lowered continuously to zero. Note that the growth rate of the CH<sub>4</sub> conversion is smaller than that of the oxygen permeation rate when both of them rise before the significant decrease. Given the sweep gas initial conditions, the fuel oxidation reactions in the gas-phase can proceed and contribute to fuel conversion and oxygen permeation only above a certain channel height. Below this channel height, oxygen permeation is governed by a non-reacting flow. To examine what results in these variations and their different growth rates, variables that are mostly dependent on the sweep gas channel height and influence the oxygen permeation rate and the CH<sub>4</sub> conversion need to be examined.

The rise of the oxygen permeation rate is attributed to the enhanced mass transfer, driven by the reaction zone established closer to it, as well as a higher transverse velocity [3]. Figure 11(a) shows that, as the sweep gas channel becomes narrower, the reaction zone is shifted towards the membrane, and the oxygen partial pressure in the immediate vicinity of the membrane first reduces and then grows significantly around  $H_{sweep} \approx 7.5mm$  at which the oxygen permeation rate suddenly drops, while the CO<sub>2</sub> concentration at the membrane surface changes to a similar degree. Beyond this point, as the sweep gas channel height is reduced further, the O<sub>2</sub> concentration near the membrane decreases again. The H<sub>2</sub>O concentration at the membrane surface remains constant and then decreases to a substantially small value. As the reaction zone approaches the membrane with decreasing the channel height, mass transfer is enhanced, reducing the O<sub>2</sub>

concentration at the membrane surface and enhancing oxygen permeation. However, the concentration of the primary product,  $H_2O$ , at the membrane surface remains constant, which does not contribute to the reduction of the  $O_2$  concentration, even if the reaction zone is established closer to the membrane. This phenomenon and the sudden increase in the magnitude of the oxygen partial pressure are explained by the low fuel concentration and the limited enhancement of the fuel oxidation reactions in the gas-phase and their extinction with a reduction of the sweep gas channel height, as shown in Figure 11(b). The gross heat release is raised with a reduction of the sweep gas channel height, enhancing the  $O_2$  consumption rate and the heat transfer towards the membrane. Note that heat transfer to the membrane increases faster than the gross heat release because of the movement of the reaction zone. Given the sweep gas initial conditions, the fuel conversion is enhanced with an increase of the oxygen permeation rate. A larger amount of the permeated oxygen promotes the fuel conversion kinetics, which enhances further oxygen consumption and thus the oxygen permeation rate. However, the gross heat release does not rise as fast as the oxygen permeation rate. In addition, as explained in Section 3.4, the low  $CH_4$  concentration results in a small rise of the  $H_2O$  concentration. Thus, although the formation of  $H_2O$  is slowly promoted (i.e., a small increase in the gross heat release), its transport towards the membrane is reduced as compared to that of  $CO_2$ , maintaining the  $H_2O$  concentration at the membrane surface constant and making the oxygen partial pressure rather dependent on the  $CO_2$  concentration. As soon as the fuel conversion is substantially limited due to the extinction of homogeneous fuel oxidation reactions, the production of  $H_2O$  and the consumption of the permeated oxygen vanish, increasing the oxygen partial pressure significantly. Therefore, along with the oxidation reactions in the gas-phase, the location of the reaction zone with respect to the membrane plays an important role in determining the extent of the mass and heat transfer and hence the oxygen permeation rate.

Extensive heat loss, a smaller residence time and the stretched flow field in the direction parallel to the membrane cause the limited enhancement of homogeneous fuel oxidation reactions and eventually lead to their extinction. Figure 11(c) shows that the residence time is gradually lowered, while the average scaled transverse velocity increases continuously, as the sweep gas channel height is reduced. In the meantime, the reaction zone temperature is lowered and drops to a small value around  $H_{sweep} \approx 7.5mm$ , coinciding with a reduction of the  $CH_4$  conversion to zero. Given a constant normal velocity of the sweep gas stream, a smaller sweep gas channel height lowers the residence time (see Eq.4) and makes the flow field more stretched in the transverse direction, resulting in a higher transverse velocity, analogous to what is seen for the sweep gas flow rate variation. Furthermore, the heat loss towards the membrane increases significantly

as the reaction zone is shifted towards the membrane. Note that the extinction of the gas-phase reactions coincides nearly with the channel height at which the reaction zone reaches the membrane. As a result of slower kinetic rates due to the heat loss from the reaction zone, the reduced residence time and the flow field more stretched in the direction parallel to the membrane, the growth of the gross heat release and accordingly the  $\text{CH}_4$  conversion is not as fast as that of the oxygen permeation rate, and the diffusion-controlled reactions extinguish at small sweep gas channel height. Thus, changing the sweep gas channel height not only affects the mass and heat transfer via the reaction zone location, it also influences the residence time and the flow field for fuel conversion processes.

#### 4. FEEDBACK INTERACTIONS

Results of the parametric analysis show that fuel conversion and oxygen permeation are strongly interconnected through the change in several dependent variables, e.g., reaction zone location relative to the membrane, oxygen consumption rate, residence time, etc. Figure 12 shows schematically the feedback interactions between the dependent variables and the oxygen permeation rate, all of which have effects on the  $\text{CH}_4$  conversion. As discussed Section 3, the sweep gas initial conditions and the reactor geometry play significant roles in influencing the local thermodynamic state and hence the fuel oxidation kinetics, affecting the gross heat release, the oxygen consumption rate and the reaction zone temperature. These in turn depend on the homogeneous fuel oxidation reactions and the flow field. In addition, the reaction zone location with respect to the membrane influences the local thermodynamic state through the mass and heat transfer towards it, changing the amount of the reaction products and thermal energy transported towards the membrane. Thus, the dependent variables encapsulating the chemical effect, the mass and heat transfer and the flow field are closely interconnected and have significant impacts on thermodynamic state at the membrane surface, i.e., the oxygen partial pressure in the immediate vicinity of the membrane and its temperature, and the oxidation kinetic rates. When the control parameters or independent variables are changed, both the chemical and heat and mass transfer effects determine the oxygen permeation rate and the  $\text{CH}_4$  conversion.

When a reactive gas is employed on the sweep side of an ITM, the local thermodynamic state changes significantly between the membrane surface and the opposite wall or sweep gas inlet, through the variations of the dependent variables by influencing the chemical reactions and the energy and species transport. The local thermodynamic

state is governed by the diffusion-controlled oxidation reactions and the mass and heat transfer in the gas-phase, and vice versa. Therefore, bulk stream parameters measured at the outlet of an ITM reactor cannot predict correctly the oxygen permeation rate and the CH<sub>4</sub> conversion in the case of an ITM reactor. To control and examine the permeation rate and the amount of fuel converted, the diffusion-controlled oxidation kinetics, the reactor geometry and mass and heat transfer have to be taken into account.

Fuel oxidation reactions in the gas-phase enable substantial fuel conversion and oxygen permeation in the absence of catalytic surface activity. The oxygen permeation rate obtained in the parametric analysis is comparable to the values reported in the literature [2], which is on the order of 0.2~9.0  $\mu\text{mol}/\text{cm}^2/\text{s}$  and based on ITM reactors, which are believed to include catalytic fuel conversion.

## 5. CONCLUSIONS

A parametric study using numerical simulations was conducted to investigate the interactions between fuel conversion and oxygen permeation on the sweep side of an ITM. Within an ITM reactor, the oxygen permeation rate is not known a priori and rather depends on the oxygen partial pressure in the immediate vicinity of the membrane and its temperature. The oxygen permeation rate, in part, determines the oxygen concentration in the reaction zone and hence the local mass ratio of oxygen to fuel, affecting fuel conversion processes. The local thermodynamic state (i.e., species concentration and temperature) govern the diffusion-controlled reactions, i.e., non-premixed reactants, and vice versa. In this study, a numerical model that incorporates detailed chemistry and species transport in the gas-phase was used, enabling us to obtain the spatially resolved profiles of species concentration, velocity and temperature. The oxygen permeation rate expression parameterized by the local oxygen partial pressure in the immediate vicinity of the membrane and its temperature was employed to relate oxygen permeation across the membrane to the local thermodynamic state. Control parameters including the fuel concentration in the sweep gas stream, its inlet temperature, flow rate and channel height were considered for the parametric study.

The oxygen permeation rate and the CH<sub>4</sub> conversion are strongly interconnected through the fuel oxidation kinetics, the reaction zone location relative to the membrane, the residence time for the chemical reactions and the oxygen

partial pressure and gas temperature near the membrane, all of which have significant effects on the local thermodynamic state and hence fuel conversion and oxygen permeation. The diffusion-controlled reactions in the gas-phase depend heavily on the local thermodynamic state and affect oxygen consumption, the heat transfer and the generation of the reaction products near the membrane, resulting in substantial fuel conversion and the enhancement of oxygen permeation even without catalytic surface activity. The location of the reaction zone relative to the membrane, governed by the fuel oxidation kinetics, has large influences on the transport of the reaction products and heat from the reaction zone towards the membrane, showing the effects of the mass and energy transfer on the local thermodynamic state near the membrane. These two effects determine the oxygen concentration in the immediate vicinity of the membrane and its temperature, respectively, and hence the oxygen permeation rate. Moreover, the heat transfer towards the membrane, i.e., heat loss from the reaction zone, impacts the reaction zone temperature and accordingly the fuel oxidation kinetics. If the heat loss is too extensive such that the reaction zone temperature is lowered to a large degree, slowing down the fuel oxidation kinetics, the extent of the chemical reactions and hence their effect on fuel conversion and oxygen permeation are significantly limited. The residence time and the flow field influence the amount of fuel that can be converted following the oxidation pathway and the heat and mass transfer away from the reaction zone. The oxygen permeation rate determines the local oxygen concentration in the reaction zone and the velocity associated with the oxidizer stream, affecting the oxidation kinetics and the reaction zone location. Sufficient oxygen permeation rate, gas temperature and the residence time are needed to support gas-phase fuel conversion processes or oxidation kinetics on the sweep side of an ITM. Thus, the feedback interactions among the reaction zone location, the residence time, the fuel oxidation kinetics and the local thermodynamic state near the membrane highlight the importance of the chemical and mass and heat transfer effect on the  $\text{CH}_4$  conversion and the oxygen permeation rate. When a reactive sweep gas is employed, the diffusion-controlled oxidation kinetics and the mass and heat transfer resistance have to be accounted for in order to examine and control the operating regimes of an ITM reactor.

## 6. ACKNOWLEDGEMENTS

The authors would like to thank the King Fahd University of Petroleum and Minerals (KFUPM) in Dhahran, Saudi Arabia, for funding the research reported in this paper through the Center of Clean Water and Clean Energy at

Massachusetts Institute of Technology and KFUPM. This work is also supported by King Abdullah University of Science and Technology grant number KSU-I1-010-01.

## 7. NOMENCLATURE

|                          |  |
|--------------------------|--|
| $x_{CH_4, sweep}$        | Fuel concentration in the sweep gas stream on a molar basis  |
| $T_{sweep}$              | Sweep gas inlet temperature  |
| $F_{sweep}$              | Sweep gas flow rate  |
| $H_{sweep}$              | Sweep gas channel height (the distance from the membrane to the sweep gas inlet or the opposite walls) |
| $J_{O_2}$                | Oxygen permeation rate   |
| $X_{CH_4}$               | CH <sub>4</sub> conversion   |
| $T_{mem}$                | Membrane temperature   |
| $P_{O_2, mem}$           | Oxygen partial pressure in the immediate vicinity of the membrane on the sweep side                    |
| $x_{k, mem}$             | The concentration of species $k$ at the membrane surface   |
| $Q_{transfer}$           | Heat transfer towards the membrane on the sweep side   |
| $Q_{gen}$                | Gross heat release from the fuel oxidation reactions   |
| $\bar{\omega}_{O_2}$     | Oxygen consumption rate  |
| $T_{max}$                | Reaction zone temperature  |
| $t_{res}$                | Residence time   |
| $U_{avg}$                | Average scaled transverse velocity   |
| $y_{front}$              | Reaction zone location relative to the membrane  |
| $y_{sweep}$              | Distance from the membrane on the sweep side   |
| $J_{O_2} / J_{CH_4, in}$ | The molar flow rate ratio of the oxygen permeation rate to the fuel influx                             |

|                       |   |
|-----------------------|---|
| $A_{air}$             | Air inlet area                                    |
| $A_{sweep}$           | Sweep gas inlet area                              |
| $L$                   | Membrane thickness                                |
| $v$                   | Normal velocity ( $y$ -direction)                 |
| $v_{O_2}$             | Normal velocity associated with oxygen permeation |
| $v_{sweep}$           | Sweep gas velocity at the sweep gas inlet         |
| $U$                   | Scaled transverse velocity ( $x$ -direction)      |
| $q$                   | Heat release rate                                 |
| $N$                   | The number of gas-phase species                   |
| $\dot{\omega}_k$      | The molar production rate of species $k$          |
| $\hat{h}_k$           | The molar enthalpy of species $k$                 |
| $V_{CH_4, converted}$ | The conversion rate of $CH_4$                     |
| $\zeta_{sweep}$       | The molar density of the sweep gas                |

## 8. REFERENCES

1. H.J.M. Bouwmeester, A.J. Burggraaf. *Chapter 10: Dense ceramic membranes for oxygen separation*, in *Fundamentals of inorganic membrane science and technology*. Burggraaf, A.J. and Cot, L., Editors. 1996, Elsevier.
2. Y. Liu, X. Tan, K. Li, *Mixed conducting ceramics for catalytic membrane processing*, Catalysis Reviews, **48** (2) (2006) 145-198.
3. J. Hong, P. Kirchen, A.F. Ghoniem, *Numerical simulation of ion transport membrane reactors: oxygen permeation and transport and fuel conversion*, Journal of Membrane Science, **407-408** (2012) 71-85.
4. R. Bredesen, K. Jordal, O. Bolland, *High-temperature membranes in power generation with  $CO_2$  capture*, Chemical Engineering and Processing, **43** (9) (2004) 1129-1158.
5. D. Bückner, D. Holmberg, T. Griffin. *Chapter 31: Techno-economic evaluation of an oxyfuel power plant using mixed conducting membranes*, in *Carbon dioxide capture for storage in deep geologic formations*. Thomas, D.C. and Benson, S.M., Editors. 2005, Elsevier.
6. S.G. Sundkvist, S. Julsrud, B. Vigeland, T. Naas, M. Budd, H. Leistner, D. Winkler, *Development and testing of AZEP reactor components*, International Journal of Greenhouse Gas Control, **1** (2) (2007) 180-187.
7. H.J.M. Bouwmeester, *Dense ceramic membranes for methane conversion*, Catalysis Today, **82** (1-4) (2003) 141-150.
8. U. Balachandran, J.T. Dusek, R.L. Mieville, R.B. Poepfel, M.S. Kleefisch, S. Pei, T.P. Kobylinski, C.A. Udovich, A.C. Bose, *Dense ceramic membranes for partial oxidation of methane to syngas*, Applied Catalysis, **133** (1) (1995) 19-29.

9. X. Tan, K. Li, *Design of mixed conducting ceramic membranes/reactors for the partial oxidation of methane to syngas*, *AIChE*, **55** (10) (2009) 2675-2685.
10. J. Hong, P. Kirchen, A.F. Ghoniem, *Laminar oxy-fuel diffusion flame supported by an oxygen-permeable-ion-transport membrane*, *Combustion and Flame*, in reviews, (2012).
11. W. Jin, X. Gu, S. Li, P. Huang, N. Xu, J. Shi, *Experimental and simulation study on a catalyst packed tubular dense membrane reactor for partial oxidation of methane to syngas*, *Chemical Engineering Science*, **55** (14) (2000) 2617-2625.
12. X. Tan, K. Li, A. Thursfield, I.S. Metcalfe, *Oxyfuel combustion using a catalytic ceramic membrane reactor*, *Catalysis Today*, **131** (1-4) (2008) 292-304.
13. W. Zhang, J. Smit, M. van Sint Annaland, J.A.M. Kuipers, *Feasibility study of a novel membrane reactor for syngas production: Part 1: Experimental study of O<sub>2</sub> permeation through perovskite membranes under reducing and non-reducing atmospheres*, *Journal of Membrane Science*, **291** (1-2) (2007) 19-32.
14. J. Smit, W. Zhang, M. van Sint Annaland, J.A.M. Kuipers, *Feasibility study of a novel membrane reactor for syngas production, Part 2: Adiabatic reactor simulations*, *Journal of Membrane Science*, **291** (1-2) (2007) 33-45.
15. S.J. Xu, W.J. Thomson, *Oxygen permeation rate through ion-conducting perovskite membranes*, *Chemical Engineering Science*, **54** (17) (1999) 3839-3850.
16. P. Kirchen, D. Apo, A. Hunt, A.F. Ghoniem, *A novel ion transport membrane reactor for fundamental investigations of oxygen permeation and oxy-combustion under reactive flow conditions*, in *Proceedings of the Combustion Institute*. 2012. <http://dx.doi.org/10.1016/j.proci.2012.07.076>.
17. R.J. Kee, M.E. Coltrin, P. Glarborg, *Chemically Reacting Flow: Theory & Practice*, Wiley-Interscience, 2003.
18. G.P. Smith, D.M. Golden, M. Frenklach, N.W. Moriarty, B. Eiteneer, M. Goldenberg, C.T. Bowman, R.K. Hanson, S. Song, W.C. Gardiner, V.V. Lissianski, Z. Qin. *GRI-Mech 3.0*. Available from: [http://www.me.berkeley.edu/gri\\_mech/](http://www.me.berkeley.edu/gri_mech/).
19. D.G. Goodwin. *Cantera*. Available from: <http://www.aresinstitute.org/Cantera/cantera-cxx.pdf>.
20. H. Tsuji, *Counterflow diffusion flames*, *Progress in Energy and Combustion Science*, **8** (2) (1982) 93-119.
21. G. Dixon-Lewis, *Structure of laminar flames*, in *Proceedings of the Combustion Institute*. 1990.
22. L. Chen, S.Z. Yong, A.F. Ghoniem, *Oxy-fuel combustion of pulverized coal: characterization, fundamentals, stabilization and CFD modeling*, *Progress in Energy and Combustion Science*, **38** (2) (2012) 156-214.
23. M.C.J. Bradford, M.A. Vannice, *CO<sub>2</sub> reforming of CH<sub>4</sub>*, *Catalysis Reviews*, **41** (1) (1999) 1-42.
24. M. Arnold, H. Wang, A. Feldhoff, *Influence of CO<sub>2</sub> on the oxygen permeation performance and the microstructure of perovskite-type (Ba<sub>0.5</sub>Sr<sub>0.5</sub>)(CO<sub>0.8</sub>Fe<sub>0.2</sub>)O<sub>3-δ</sub> membranes*, *Journal of Membrane Science*, **293** (1-2) (2007) 44-52.
25. O. Czuprat, M. Arnold, S. Schirrmeister, T. Schiestel, J. Caro, *Influence of CO<sub>2</sub> on the oxygen permeation performance of perovskite-type BaCO<sub>x</sub>Fe<sub>y</sub>Zr<sub>z</sub>O<sub>3-δ</sub> hollow fiber membranes*, *Journal of Membrane Science*, **364** (1-2) (2010) 132-137.
26. J. Sunarso, S. Baumann, J.M. Serra, W.A. Meulenbergh, S. Liu, Y.S. Lin, J.C. Diniz da Costa, *Mixed ionic-electronic conducting (MIEC) ceramic-based membranes for oxygen separation*, *Journal of Membrane Science*, **320** (1-2) (2008) 13-41.
27. P. Popp, M. Baum, *Analysis of wall heat fluxes, reaction mechanisms, and unburnt hydrocarbons during the head-on quenching of a laminar methane flame*, *Combustion and Flame*, **108** (3) (1997) 327-348.
28. I.S. Wichman, *On diffusion flame attachment near cold surfaces*, *Combustion and Flame*, **117** (1-2) (1999) 384-393.



## List of Figures

- FIGURE 1 THE STAGNATION-FLOW CONFIGURATION CONSIDERED IN THIS INVESTIGATION (  $U$  = NORMAL VELOCITY (  $y$  -DIRECTION),  $U$  = SCALED TRANSVERSE VELOCITY (  $x$  -DIRECTION),  $x_{CH_4, sweep}$  = FUEL CONCENTRATION IN THE SWEEP GAS ON A MOLAR BASIS,  $T_{sweep}$  = SWEEP GAS INLET TEMPERATURE,  $F_{sweep}$  = SWEEP GAS FLOW RATE,  $H_{sweep}$  = SWEEP GAS CHANNEL HEIGHT,  $t_{mem}$  = MEMBRANE THICKNESS, AIR INLET AREA =  $A_{air} = 5.33 \times 10^{-3} m^2$ , SWEEP GAS INLET AREA =  $A_{sweep} = 5.81 \times 10^{-3} m^2$  )
- FIGURE 2 BASE-CASE (  $x_{CH_4, sweep} = 6\%$ ,  $T_{sweep} = 1300K$ ,  $F_{sweep} = 4.39 \times 10^{-4} m^3/s$  AND  $H_{sweep} = 25.4mm$  )  
RESULTS: (A) THE PROFILES OF THE TEMPERATURE, THE HEAT RELEASE RATE, THE  $CH_4$  AND  $O_2$  MOLE FRACTIONS; (B) THE CONCENTRATIONS OF THE PRODUCTS INCLUDING  $CO_2$ ,  $CO$ ,  $H_2O$  AND  $H_2$ , ALONG THE DIRECTION NORMAL TO THE MEMBRANE
- FIGURE 3 THE DEPENDENCY OF THE OXYGEN PERMEATION RATE AND THE  $CH_4$  CONVERSION ON THE FUEL CONCENTRATION (  $T_{sweep} = 1300K$ ,  $F_{sweep} = 4.39 \times 10^{-4} m^3/s$  AND  $H_{sweep} = 25.4mm$  )
- FIGURE 4 THE VARIATIONS OF: (A) THE OXYGEN CONSUMPTION RATE, THE GROSS HEAT RELEASE FROM THE CHEMICAL REACTIONS, THE REACTION ZONE LOCATION RELATIVE TO THE MEMBRANE AND THE MOLAR FLOW RATE RATIO OF THE OXYGEN PERMEATION RATE TO THE FUEL INFLUX; (B) THE HEAT TRANSFER TOWARDS THE MEMBRANE, THE MEMBRANE TEMPERATURE AND THE CONCENTRATIONS OF  $H_2O$  AND  $O_2$  AT THE MEMBRANE SURFACE, WITH RESPECT TO THE CHANGE IN THE FUEL CONCENTRATION (  $T_{sweep} = 1300K$ ,  $F_{sweep} = 4.39 \times 10^{-4} m^3/s$  AND  $H_{sweep} = 25.4mm$  )
- FIGURE 5 (A) THE VARIATIONS OF THE REACTION ZONE TEMPERATURE, THE GROSS HEAT RELEASE SUBTRACTED BY THE HEAT TRANSFER TOWARDS THE MEMBRANE AND THE CONCENTRATIONS OF  $CH_4$ ,  $CO$ ,  $H_2$  AT THE MEMBRANE SURFACE, WITH RESPECT TO THE CHANGE IN THE FUEL CONCENTRATION; (B) THE PROFILES OF THE HEAT RELEASE RATE AT DIFFERENCE FUEL CONCENTRATIONS (  $T_{sweep} = 1300K$ ,  $F_{sweep} = 4.39 \times 10^{-4} m^3/s$  AND  $H_{sweep} = 25.4mm$  )
- FIGURE 6 THE DEPENDENCY OF THE OXYGEN PERMEATION RATE AND THE  $CH_4$  CONVERSION ON THE SWEEP GAS INLET TEMPERATURE (  $x_{CH_4, sweep} = 6\%$ ,  $F_{sweep} = 4.39 \times 10^{-4} m^3/s$  AND  $H_{sweep} = 25.4mm$  )
- FIGURE 7 THE VARIATIONS OF: (A) THE GROSS HEAT RELEASE FROM THE CHEMICAL REACTIONS AND THE OXYGEN CONSUMPTION RATE; (B) THE MEMBRANE TEMPERATURE, THE CONCENTRATIONS OF  $H_2O$  AND  $O_2$  AT THE MEMBRANE SURFACE, THE REACTION ZONE LOCATION RELATIVE TO THE MEMBRANE AND THE HEAT TRANSFER TOWARDS THE MEMBRANE, WITH RESPECT TO THE CHANGE IN THE SWEEP GAS INLET TEMPERATURE (  $x_{CH_4, sweep} = 6\%$ ,  $F_{sweep} = 4.39 \times 10^{-4} m^3/s$  AND  $H_{sweep} = 25.4mm$  )
- FIGURE 8 THE CHANGE IN THE OXYGEN PERMEATION RATE AND THE  $CH_4$  CONVERSION, WHEN THE SWEEP GAS FLOW RATE IS RAISED (  $x_{CH_4, sweep} = 6\%$ ,  $T_{sweep} = 1300K$  AND  $H_{sweep} = 25.4mm$  )
- FIGURE 9 THE VARIATIONS OF: (A) THE CONCENTRATIONS OF  $CO_2$ ,  $H_2O$  AND  $O_2$  AT THE MEMBRANE SURFACE AND THE REACTION ZONE LOCATION RELATIVE TO THE MEMBRANE; (B) THE GROSS HEAT RELEASE FROM THE CHEMICAL REACTIONS, THE OXYGEN CONSUMPTION RATE, THE HEAT TRANSFER TOWARDS THE MEMBRANE AND THE MOLAR FLOW RATE RATIO OF THE OXYGEN PERMEATION RATE TO THE FUEL INFLUX; (C) THE RESIDENCE TIME, THE REACTION ZONE TEMPERATURE AND THE AVERAGE SCALED TRANSVERSE VELOCITY, WITH RESPECT TO THE CHANGE IN THE SWEEP GAS FLOW RATE (  $x_{CH_4, sweep} = 6\%$ ,  $T_{sweep} = 1300K$  AND  $H_{sweep} = 25.4mm$  )
- FIGURE 10 THE DEPENDENCY OF THE OXYGEN PERMEATION RATE AND THE  $CH_4$  CONVERSION ON THE SWEEP GAS CHANNEL HEIGHT (  $x_{CH_4, sweep} = 6\%$ ,  $T_{sweep} = 1300K$  AND  $F_{sweep} = 4.39 \times 10^{-4} m^3/s$  )
- FIGURE 11 THE CHANGE IN: (A) THE CONCENTRATIONS OF  $CO_2$ ,  $H_2O$  AND  $O_2$  AT THE MEMBRANE SURFACE AND THE REACTION ZONE LOCATION RELATIVE TO THE MEMBRANE; (B) THE GROSS HEAT RELEASE FROM THE CHEMICAL REACTIONS, THE OXYGEN CONSUMPTION RATE AND THE HEAT TRANSFER TOWARDS THE MEMBRANE; (C) THE RESIDENCE TIME, THE REACTION ZONE TEMPERATURE AND THE AVERAGE SCALED TRANSVERSE VELOCITY, WHEN THE SWEEP GAS CHANNEL HEIGHT IS REDUCED (  $x_{CH_4, sweep} = 6\%$ ,  $T_{sweep} = 1300K$  AND  $F_{sweep} = 4.39 \times 10^{-4} m^3/s$  )
- FIGURE 12 THE FEEDBACK INTERACTIONS AMONG IMPORTANT DEPENDENT VARIABLES AFFECTING THE OXYGEN PERMEATION RATE AND THE  $CH_4$  CONVERSION WITH RESPECT TO THE VARIATION OF THE CONTROL PARAMETERS OR INDEPENDENT VARIABLES

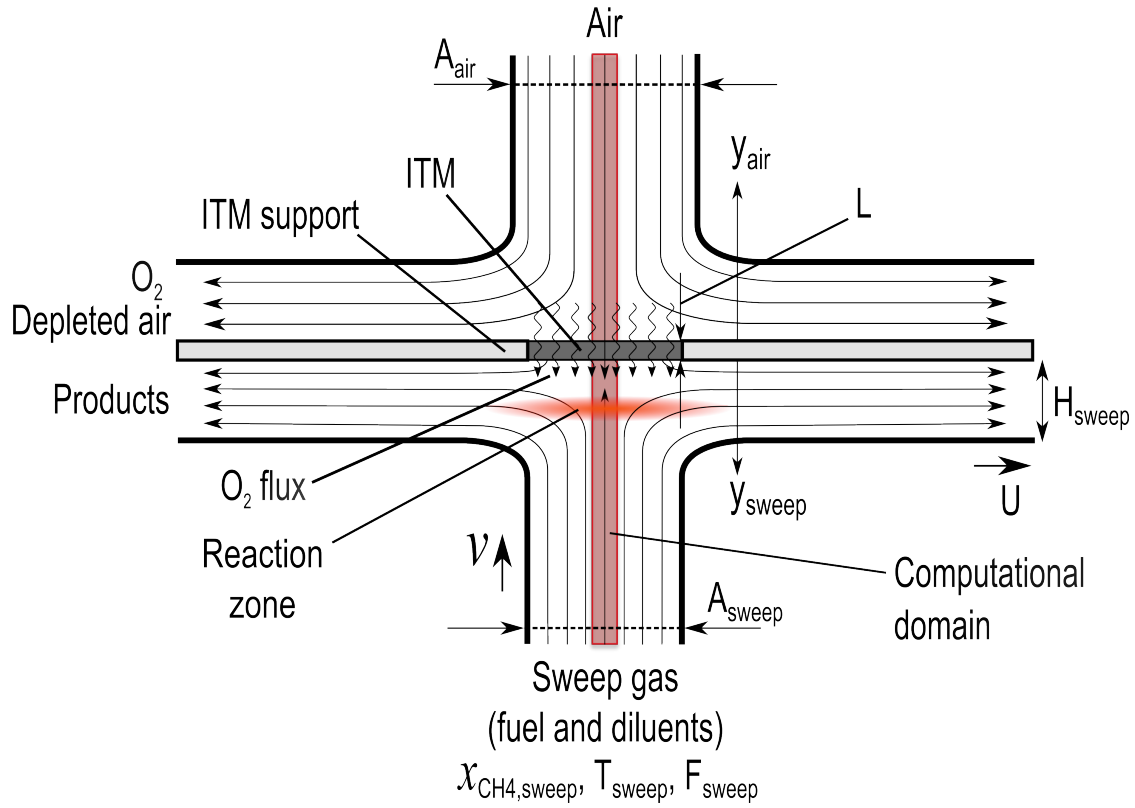
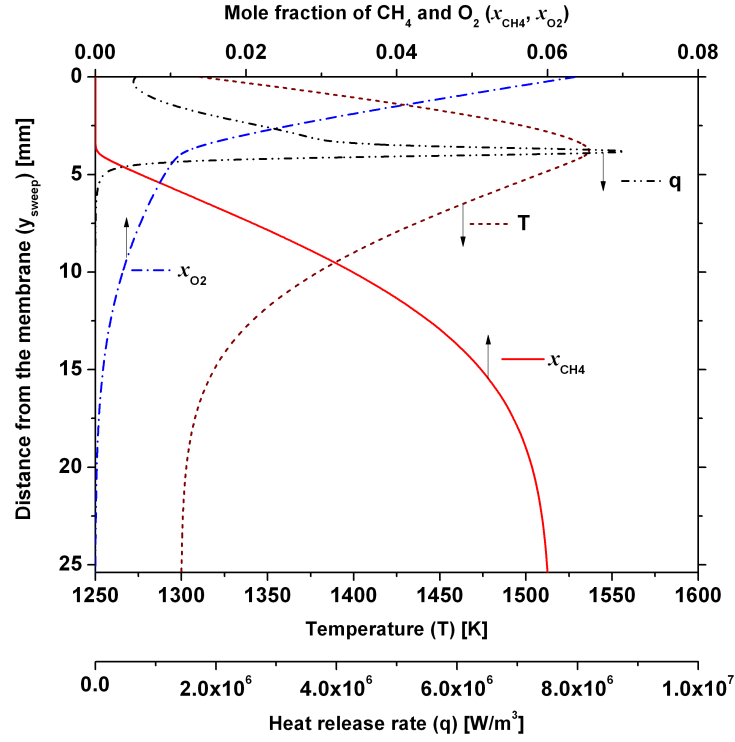
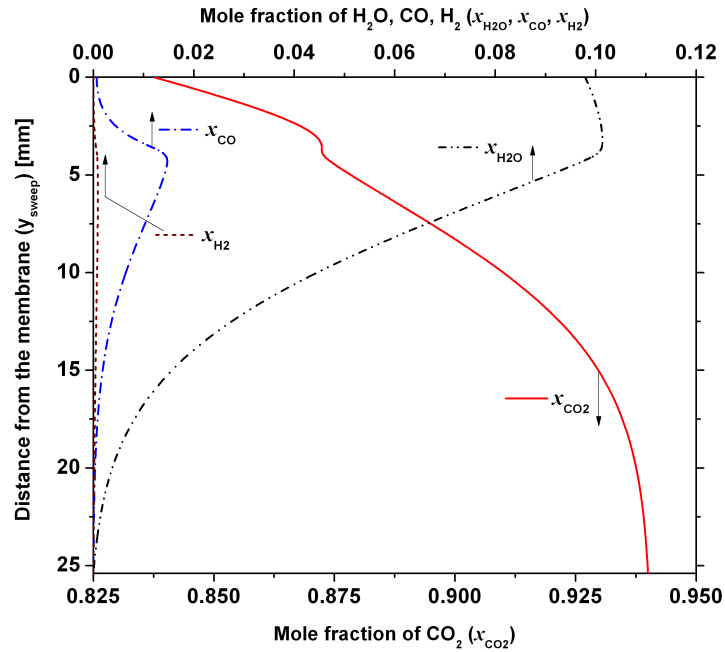


**Figure 1** The stagnation-flow configuration considered in this investigation ( $v$  = normal velocity ( $y$ -direction),  $U$  = scaled transverse velocity ( $x$ -direction),  $x_{CH_4,sweep}$  = fuel concentration in the sweep gas on a molar basis,  $T_{sweep}$  = sweep gas inlet temperature,  $F_{sweep}$  = sweep gas flow rate,  $H_{sweep}$  = sweep gas channel height,  $t_{mem}$  = membrane thickness, air inlet area =  $A_{air} = 5.33 \times 10^{-3} m^2$ , sweep gas inlet area =  $A_{sweep} = 5.81 \times 10^{-3} m^2$ )



(a)



(b)

Figure 2 Base-case ( $x_{\text{CH}_4, \text{sweep}} = 6\%$ ,  $T_{\text{sweep}} = 1300\text{K}$ ,  $F_{\text{sweep}} = 4.39 \times 10^{-4} \text{ m}^3/\text{s}$  and  $H_{\text{sweep}} = 25.4\text{mm}$ )

results: (a) the profiles of the temperature, the heat release rate, the  $\text{CH}_4$  and  $\text{O}_2$  mole fractions; (b) the concentrations of the products including  $\text{CO}_2$ ,  $\text{CO}$ ,  $\text{H}_2\text{O}$  and  $\text{H}_2$ , along the direction normal to the membrane

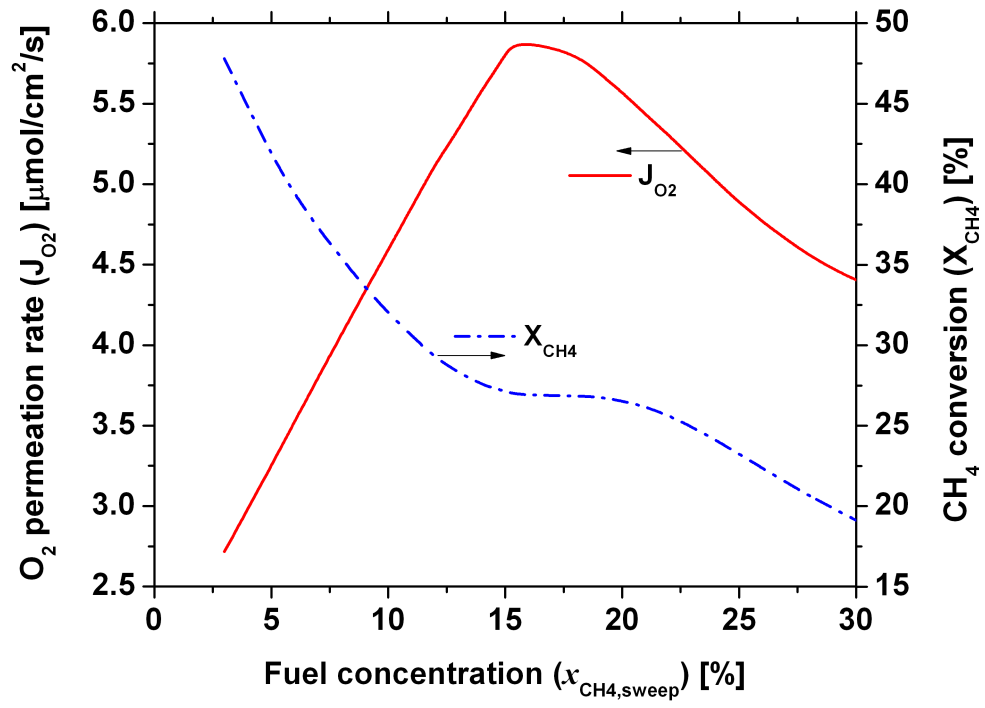
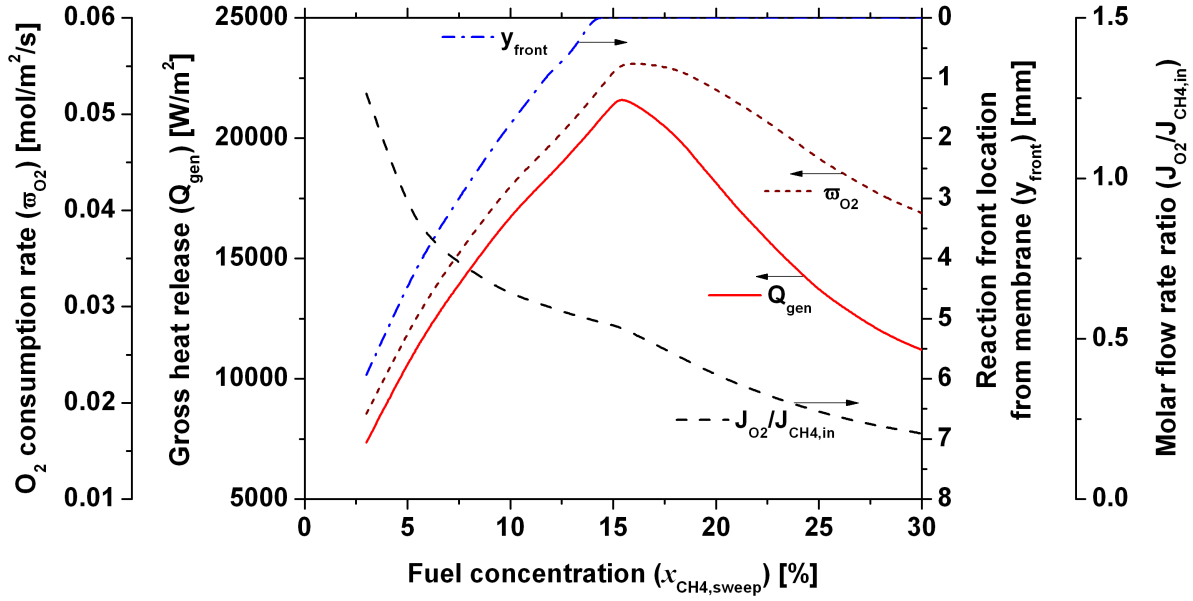
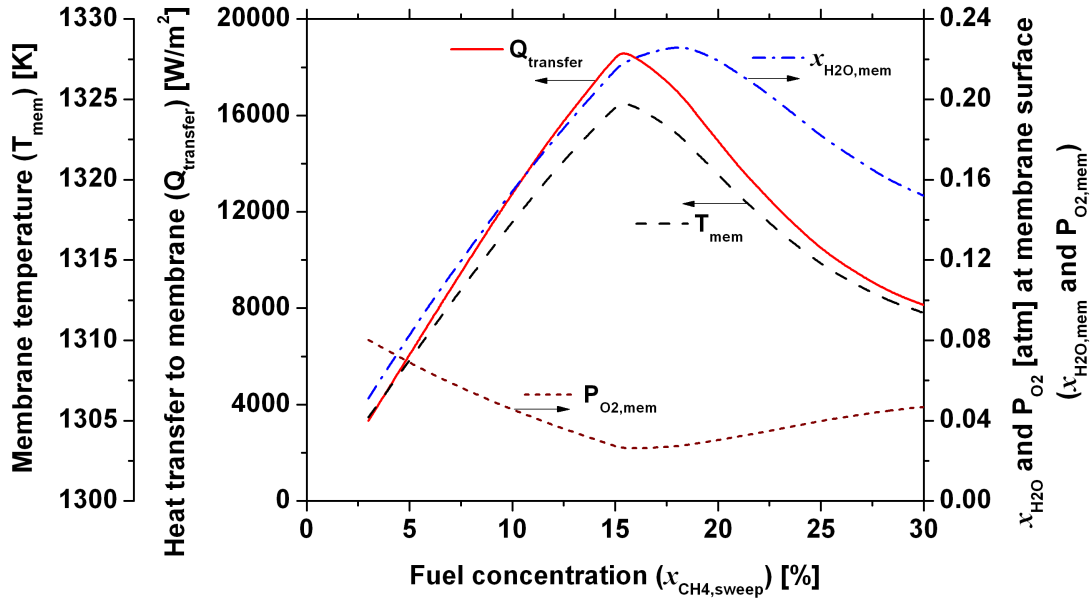


Figure 3 The dependency of the oxygen permeation rate and the  $CH_4$  conversion on the fuel concentration (  $T_{sweep} = 1300K$  ,  $F_{sweep} = 4.39 \times 10^{-4} m^3/s$  and  $H_{sweep} = 25.4mm$  )



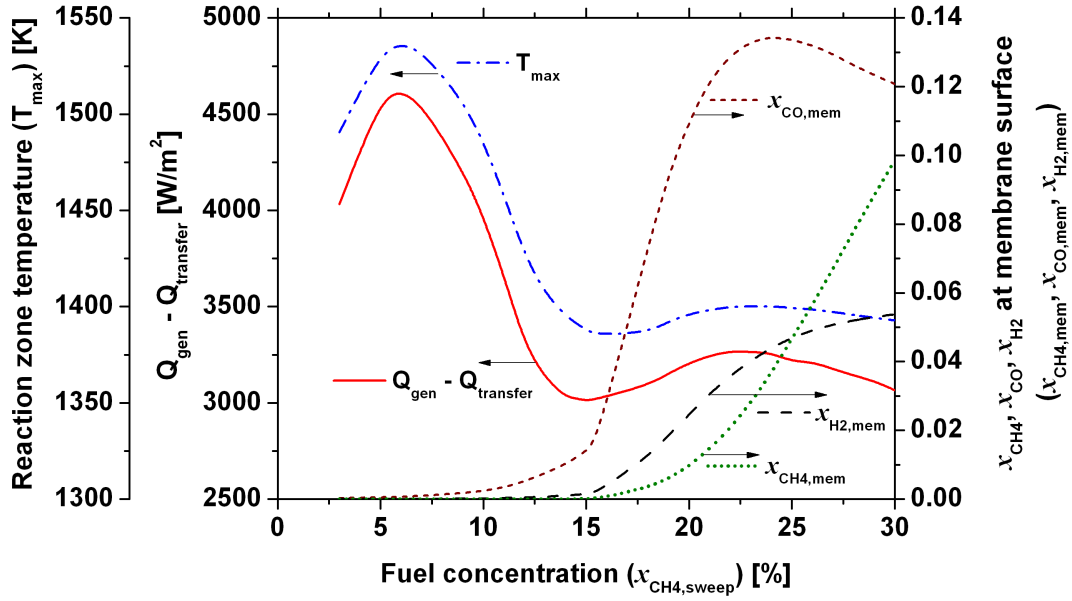
(a)



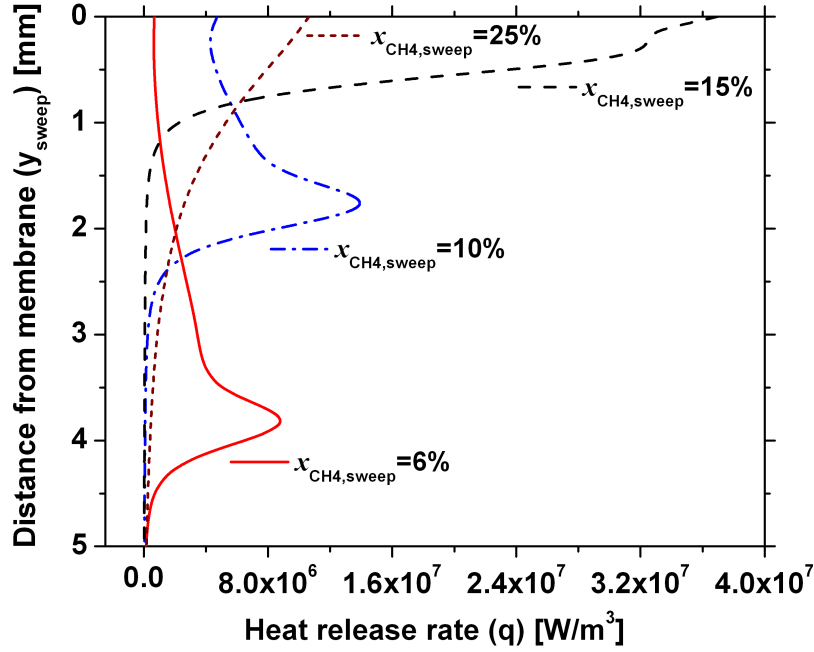
(b)

Figure 4 The variations of: (a) the oxygen consumption rate, the gross heat release from the chemical reactions, the reaction zone location relative to the membrane and the molar flow rate ratio of the oxygen permeation rate to the fuel influx; (b) the heat transfer towards the membrane, the membrane temperature and the concentrations of H<sub>2</sub>O and O<sub>2</sub> at the membrane surface, with respect to the change in the fuel concentration ( $T_{sweep} = 1300 K$ ,

$$F_{sweep} = 4.39 \times 10^{-4} m^3/s \text{ and } H_{sweep} = 25.4 mm)$$



(a)



(b)

Figure 5 (a) The variations of the reaction zone temperature, the gross heat release subtracted by the heat transfer towards the membrane and the concentrations of CH<sub>4</sub>, CO, H<sub>2</sub> at the membrane surface, with respect to the change in the fuel concentration; (b) the profiles of the heat release rate at difference fuel concentrations ( $T_{sweep} = 1300\text{ K}$ ,

$$F_{sweep} = 4.39 \times 10^{-4} \text{ m}^3/\text{s} \text{ and } H_{sweep} = 25.4 \text{ mm})$$

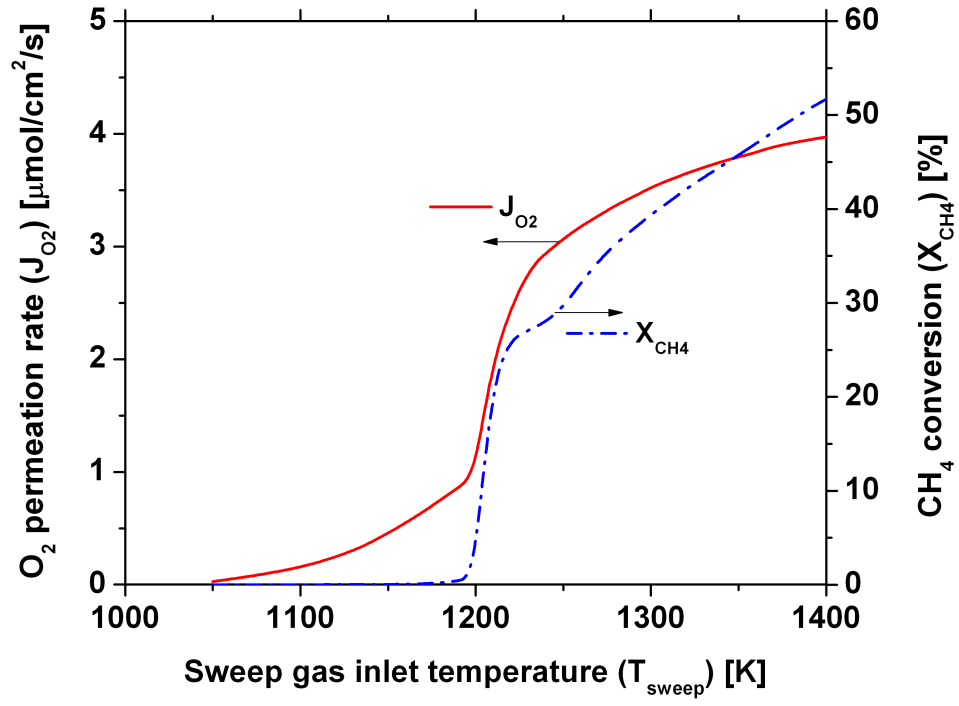
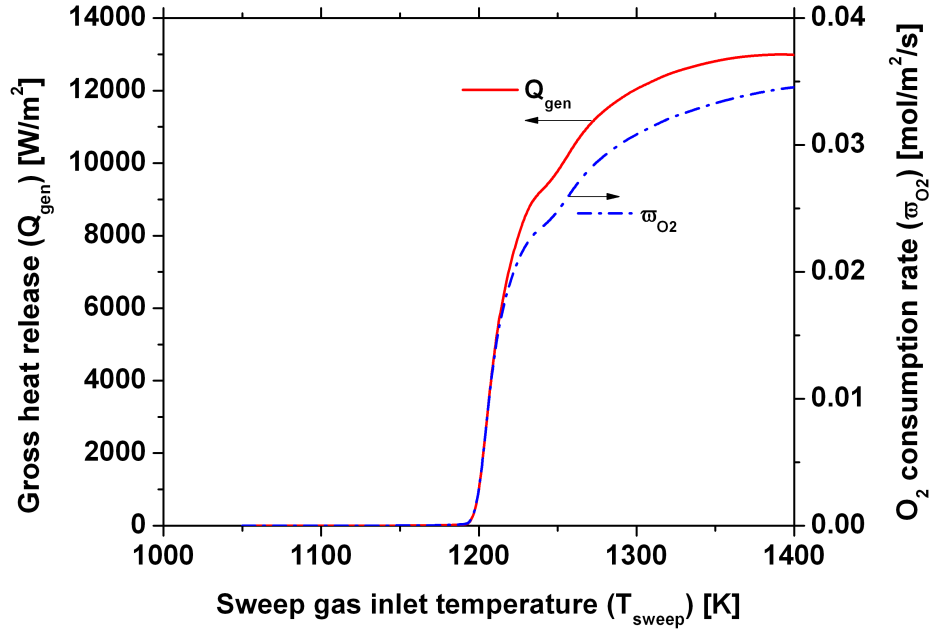
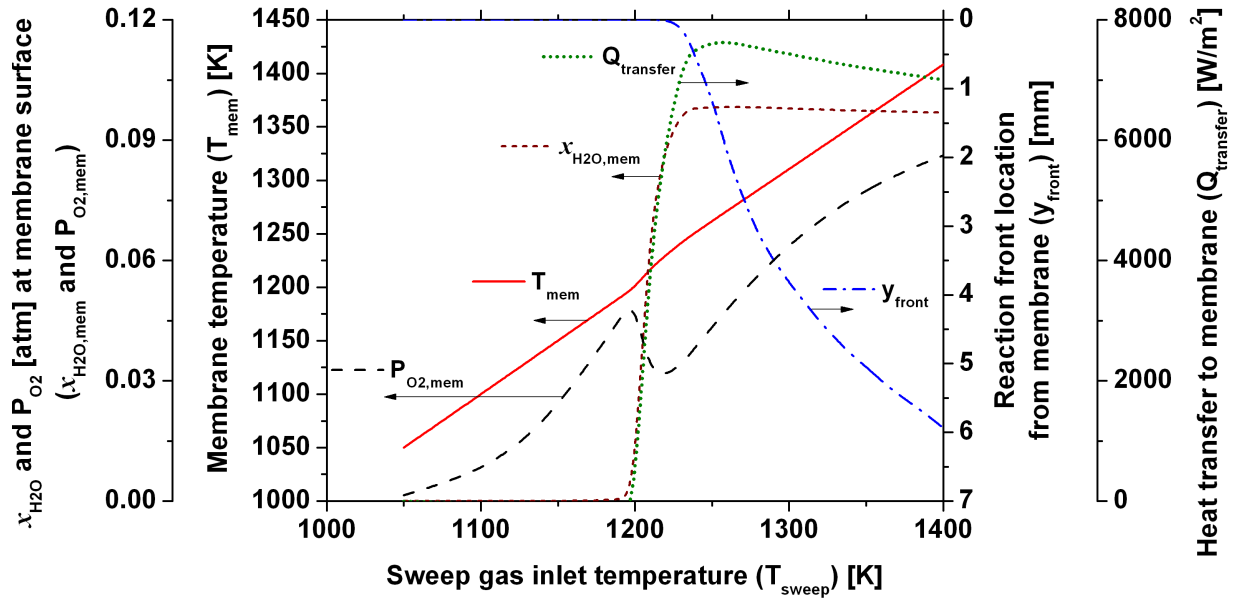


Figure 6 The dependency of the oxygen permeation rate and the CH<sub>4</sub> conversion on the sweep gas inlet temperature

( $x_{\text{CH}_4, \text{sweep}} = 6\%$ ,  $F_{\text{sweep}} = 4.39 \times 10^{-4} \text{ m}^3/\text{s}$  and  $H_{\text{sweep}} = 25.4 \text{ mm}$ )



(a)



(b)

Figure 7 The variations of: (a) the gross heat release from the chemical reactions and the oxygen consumption rate; (b) the membrane temperature, the concentrations of  $\text{H}_2\text{O}$  and  $\text{O}_2$  at the membrane surface, the reaction zone location relative to the membrane and the heat transfer towards the membrane, with respect to the change in the sweep gas inlet temperature ( $x_{\text{CH}_4,\text{sweep}} = 6\%$ ,  $F_{\text{sweep}} = 4.39 \times 10^{-4} \text{ m}^3/\text{s}$  and  $H_{\text{sweep}} = 25.4 \text{ mm}$ )



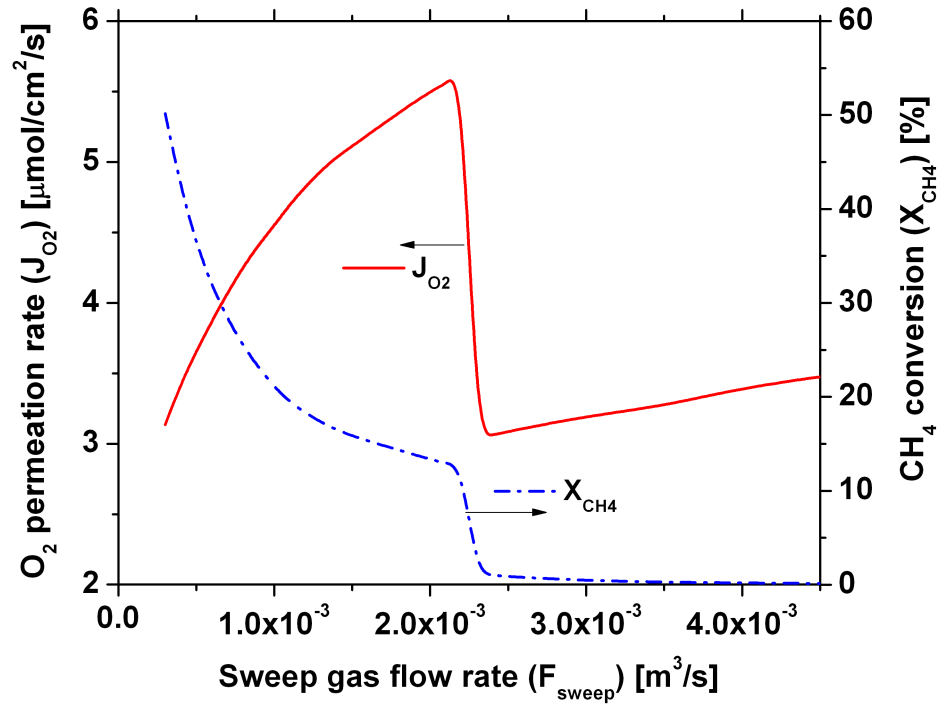
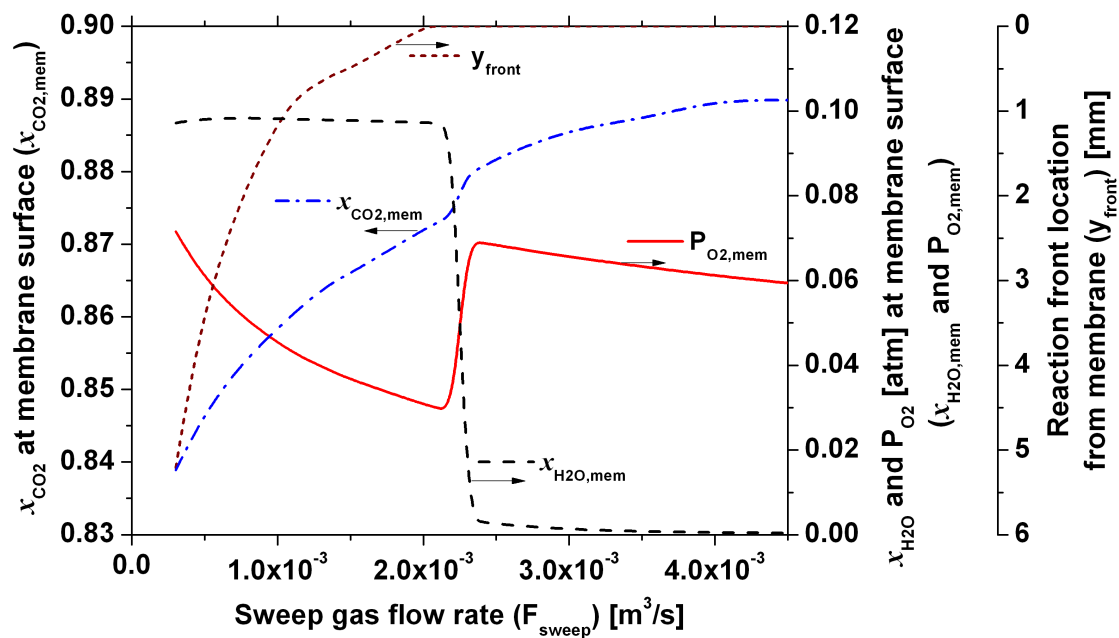
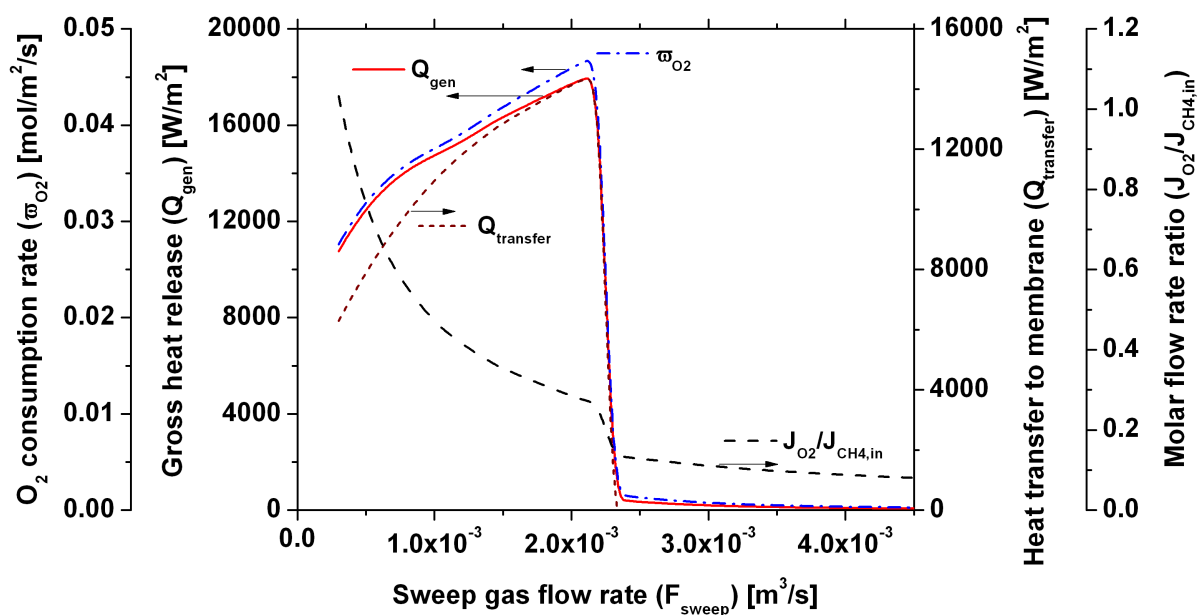


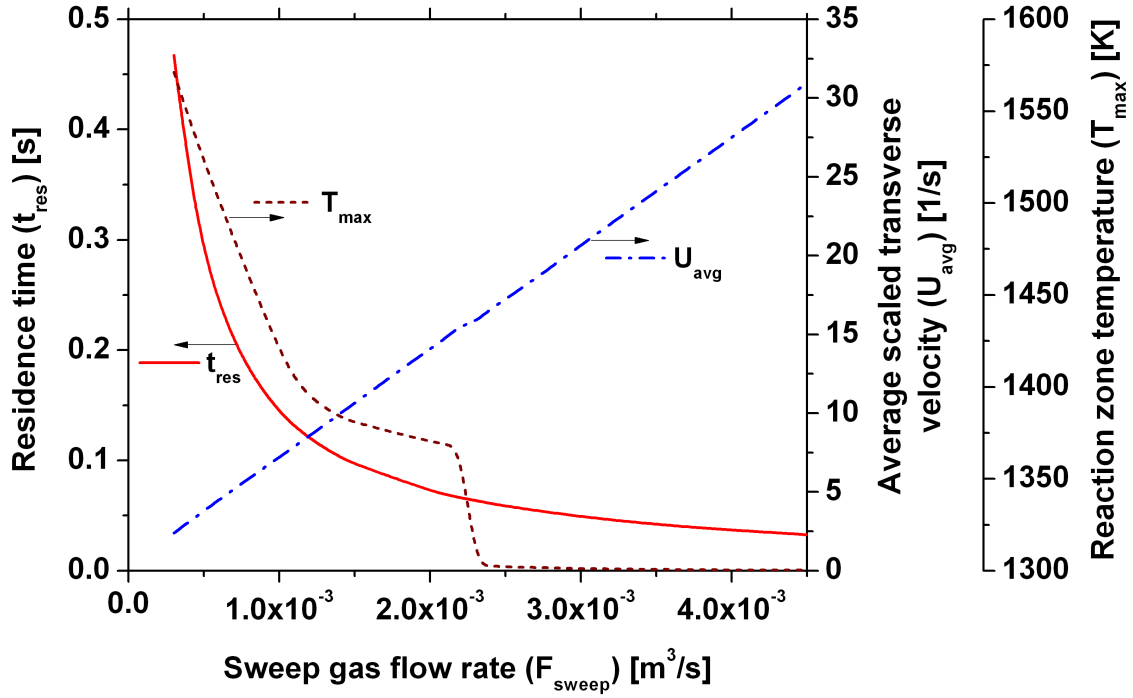
Figure 8 The change in the oxygen permeation rate and the CH<sub>4</sub> conversion, when the sweep gas flow rate is raised (  $x_{\text{CH}_4, \text{sweep}} = 6\%$ ,  $T_{\text{sweep}} = 1300\text{K}$  and  $H_{\text{sweep}} = 25.4\text{mm}$  )



(a)



(b)



(c)

Figure 9 The variations of: (a) the concentrations of  $\text{CO}_2$ ,  $\text{H}_2\text{O}$  and  $\text{O}_2$  at the membrane surface and the reaction zone location relative to the membrane; (b) the gross heat release from the chemical reactions, the oxygen consumption rate, the heat transfer towards the membrane and the molar flow rate ratio of the oxygen permeation rate to the fuel influx; (c) the residence time, the reaction zone temperature and the average scaled transverse velocity, with respect to the change in the sweep gas flow rate ( $x_{\text{CH}_4, \text{sweep}} = 6\%$ ,  $T_{\text{sweep}} = 1300\text{K}$  and  $H_{\text{sweep}} = 25.4\text{mm}$ )

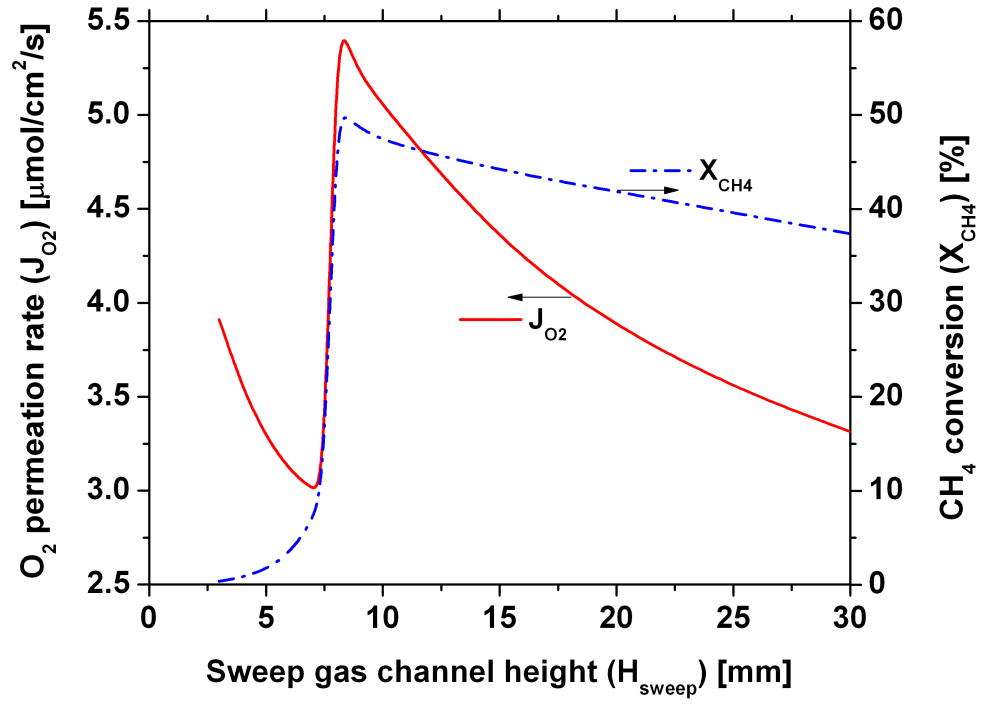
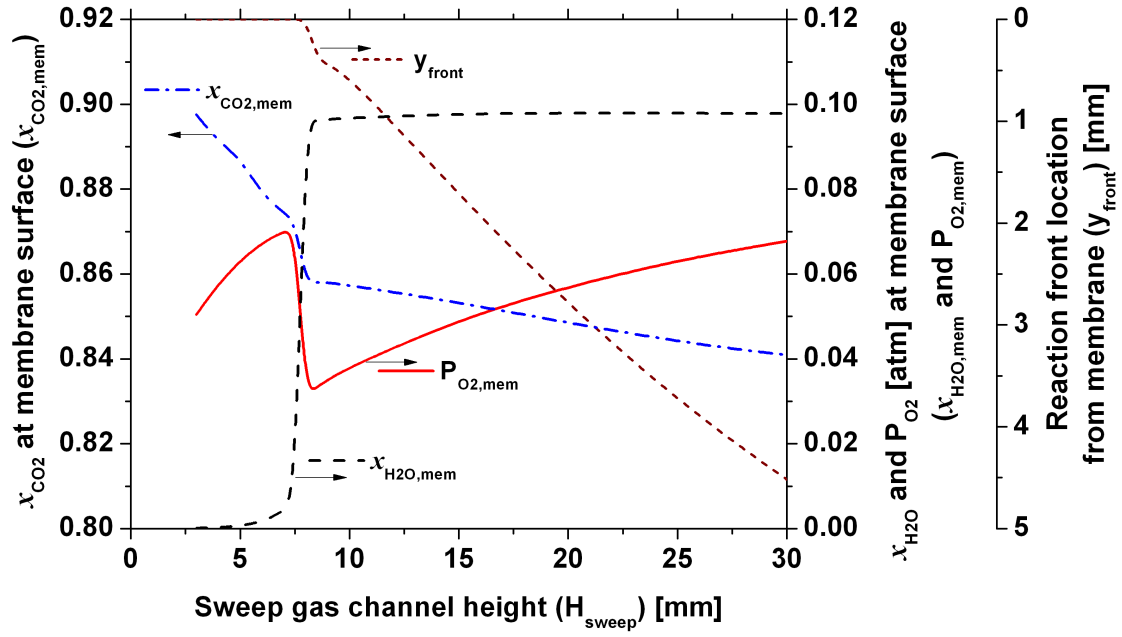
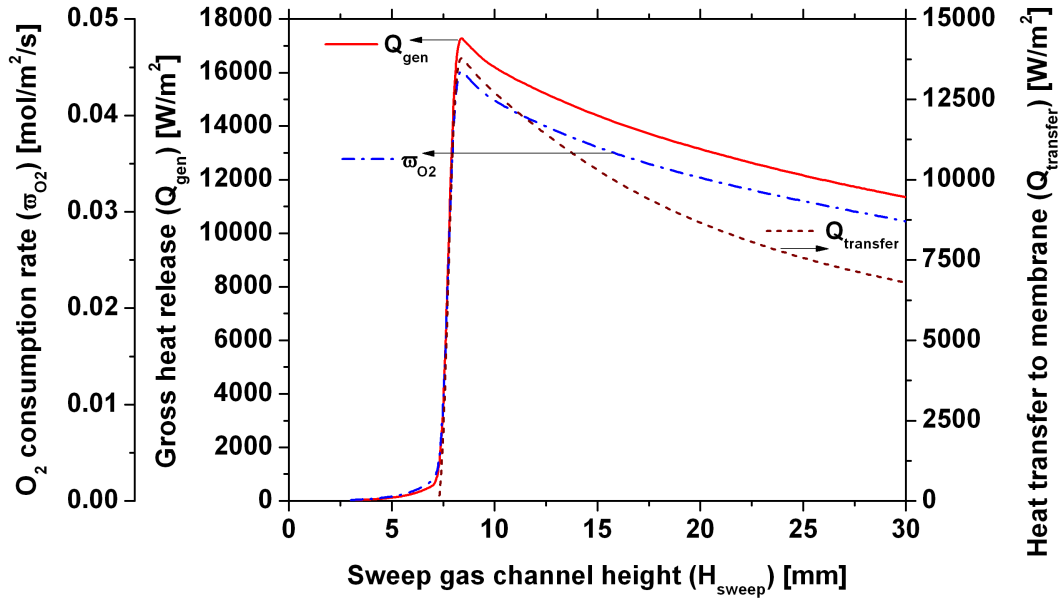


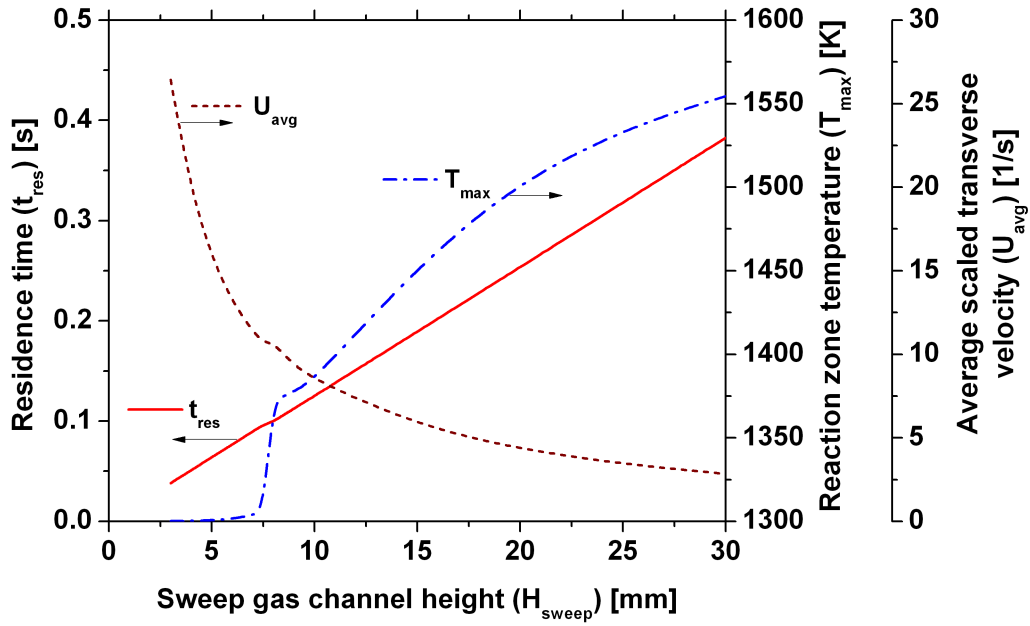
Figure 10 The dependency of the oxygen permeation rate and the  $\text{CH}_4$  conversion on the sweep gas channel height (  $x_{CH_4, sweep} = 6\%$  ,  $T_{sweep} = 1300K$  and  $F_{sweep} = 4.39 \times 10^{-4} m^3/s$  )



(a)



(b)



(c)

Figure 11 The change in: (a) the concentrations of  $\text{CO}_2$ ,  $\text{H}_2\text{O}$  and  $\text{O}_2$  at the membrane surface and the reaction zone location relative to the membrane; (b) the gross heat release from the chemical reactions, the oxygen consumption rate and the heat transfer towards the membrane; (c) the residence time, the reaction zone temperature and the average scaled transverse velocity, when the sweep gas channel height is reduced ( $x_{\text{CH}_4, \text{sweep}} = 6\%$ ,

$$T_{\text{sweep}} = 1300\text{K} \text{ and } F_{\text{sweep}} = 4.39 \times 10^{-4} \text{ m}^3/\text{s})$$

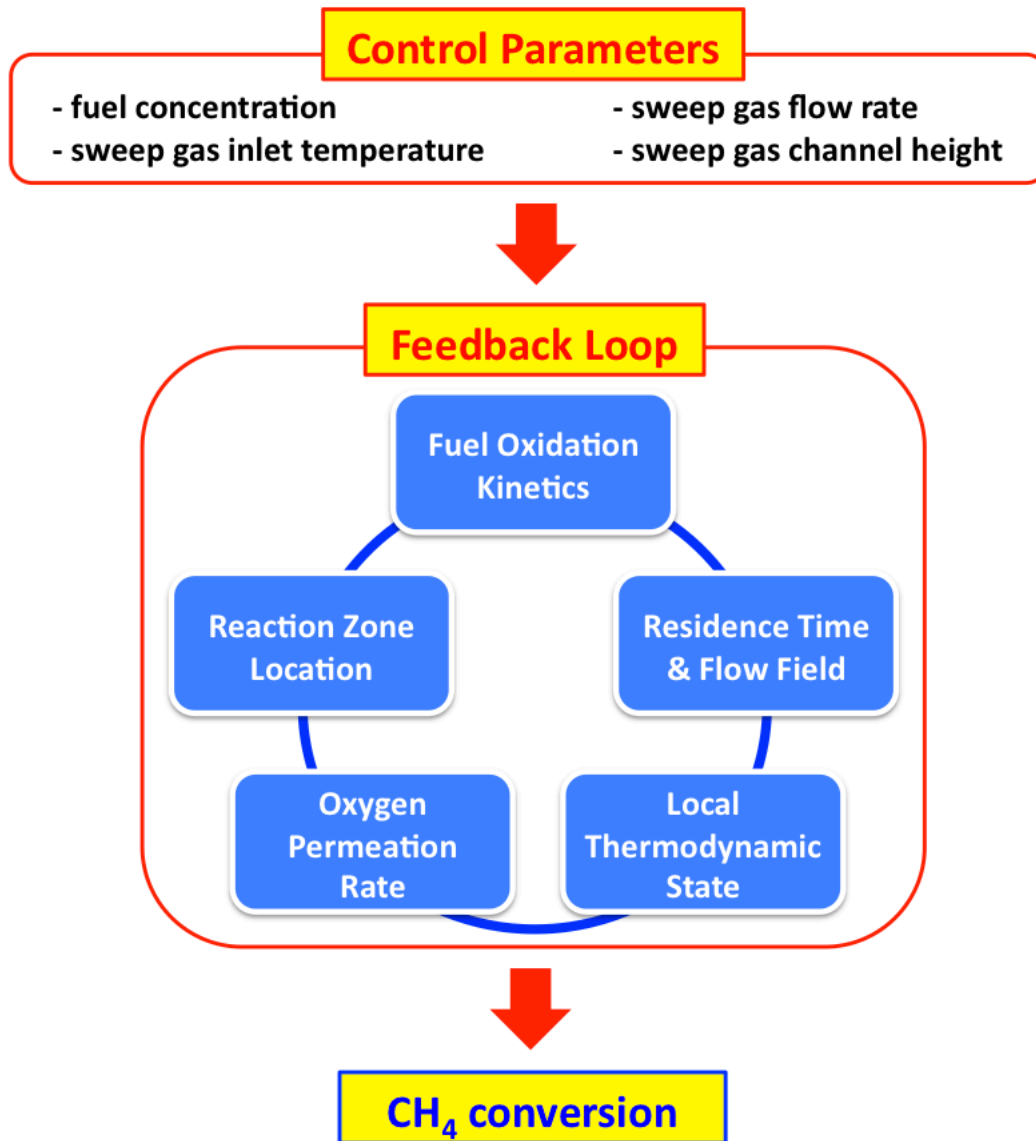


Figure 12 The feedback interactions among important dependent variables affecting the oxygen permeation rate and the  $\text{CH}_4$  conversion with respect to the variation of the control parameters or independent variables

## List of Tables

TABLE 1 THE CONTROL PARAMETERS OR INDEPENDENT VARIABLES AND THEIR VARIATIONS CONSIDERED IN THE PARAMETRIC STUDY



**Table 1 The control parameters or independent variables and their variations considered in the parametric study**

| Control parameter<br>(independent variable)                                     |                   | Unit                | Base-case value       | Range of variations   |                       |
|---|-------------------|---------------------|-----------------------|-----------------------|-----------------------|
|   |                   |                     |                       | Min                   | Max                   |
| Fuel concentration in the sweep gas (with the remainder being CO <sub>2</sub> ) | $x_{CH_4, sweep}$ | [%]                 | 6                     | 3                     | 30                    |
| Sweep gas inlet temperature   | $T_{sweep}$       | [K]                 | 1300                  | 1050                  | 1400                  |
| Sweep gas flow rate   | $F_{sweep}$       | [m <sup>3</sup> /s] | $4.39 \times 10^{-4}$ | $3.00 \times 10^{-4}$ | $4.50 \times 10^{-3}$ |
| Sweep gas channel height  | $H_{sweep}$       | [mm]                | 25.4                  | 3.00                  | 30.0                  |